

AperTO - Archivio Istituzionale Open Access dell'Università di Torino

**Veblenite,  $K_2\text{-}2\text{Na}(\text{Fe}^{2+5}\text{Fe}^{3+4}\text{Mn}^{2+7})\text{Nb}_3\text{Ti}(\text{Si}_2\text{O}_7)_2(\text{Si}_8\text{O}_{22})_2\text{O}_6(\text{OH})_{10}(\text{H}_2\text{O})_3$ , a new mineral from Seal Lake, Newfoundland and Labrador: mineral description, crystal structure, and a new veblenite ( $\text{Si}_8\text{O}_{22}$ ) ribbon**

**This is the author's manuscript**

*Original Citation:*

*Availability:*

This version is available <http://hdl.handle.net/2318/142931> since

*Published version:*

DOI:10.1180/minmag.2013.077.7.06

*Terms of use:*

Open Access

Anyone can freely access the full text of works made available as "Open Access". Works made available under a Creative Commons license can be used according to the terms and conditions of said license. Use of all other works requires consent of the right holder (author or publisher) if not exempted from copyright protection by the applicable law.

(Article begins on next page)

Revision 1

1  
2  
3  
4  
5  
6  
7 **Veblenite,  $K_2\Box_2Na(Fe^{2+}_5Fe^{3+}_4Mn^{2+}_7\Box)Nb_3Ti(Si_2O_7)_2(Si_8O_{22})_2O_6(OH)_{10}(H_2O)_3$ , a new mineral**  
8 **from Seal Lake, Newfoundland and Labrador: mineral description, crystal structure, and**  
9 **a new veblenite ( $Si_8O_{22}$ ) ribbon.**

10  
11  
12  
13 F. Cámara<sup>1,2,3\*</sup>, E. Sokolova<sup>3</sup>, F.C. Hawthorne<sup>3</sup>, R. Rowe<sup>4</sup>, J.D. Grice<sup>4</sup> and K.T. Tait<sup>5</sup>

14  
15 <sup>1</sup> *Dipartimento di Scienze della Terra, Università degli Studi di Torino, via Valperga Caluso 35,*  
16 *10125 Torino, Italy*

17  
18 <sup>2</sup> *CrisDi, Interdepartmental Centre for the Research and Development of Crystallography, Via P.*  
19 *Giuria 5, I-10125, Torino, Italy*

20  
21 <sup>3</sup> *Department of Geological Sciences, University of Manitoba, 240 Wallace Building, 125 Dysart*  
22 *Road, Winnipeg, Manitoba R3T 2N2, Canada*

23  
24 <sup>4</sup> *Research Division, Canadian Museum of Nature, 240 McLeod St, Ottawa, ON K2P 2R,*  
25 *Ontario, Canada*

26  
27 <sup>5</sup> *Department of Natural History, Royal Ontario Museum, 100 Queens Park, Toronto, ON M5S*  
28 *2C6, Ontario Canada*

29  
30  
31  
32 \* Corresponding author, E-mail address: fernando.camaraartigas@unito.it

33

34 **Abstract**

35 Veblenite, ideally  $K_2\Box_2Na(Fe^{2+}_5Fe^{3+}_4Mn^{2+}_7\Box)Nb_3Ti(Si_2O_7)_2(Si_8O_{22})_2O_6(OH)_{10}(H_2O)_3$ , is a new  
36 mineral with no natural or synthetic analogues. The mineral occurs at Ten Mile Lake, Seal Lake  
37 area, Newfoundland and Labrador (Canada), in a band of paragneiss consisting chiefly of albite  
38 and arfvedsonite. Veblenite occurs as red brown single laths and fibres included in feldspar.  
39 Associated minerals are niobophyllite, albite, arfvedsonite, aegirine-augite, barylite, eudidymite,  
40 neptunite, Mn-rich pectolite, pyrochlore, sphalerite and galena. Veblenite has perfect cleavage  
41 on {001} and splintery fracture. Its calculated density is  $3.046\text{ g cm}^{-3}$ . Veblenite is biaxial  
42 negative with  $\alpha\ 1.676(2)$ ,  $\beta\ 1.688(2)$ ,  $\gamma\ 1.692(2)$  ( $\lambda\ 590\text{ nm}$ ),  $2V_{\text{meas}} = 65(1)^\circ$ ,  $2V_{\text{calc}} = 59.6^\circ$ , with  
43 no discernible dispersion. It is pleochroic in the following pattern:  $X = \text{black}$ ,  $Y = \text{black}$ ,  $Z =$   
44 orange-brown. The mineral is red-brown with a vitreous, translucent luster and very pale brown  
45 streak. It does not fluoresce under short and long-wave UV-light. Veblenite is triclinic, space  
46 group  $P\bar{1}$ ,  $a\ 5.3761(3)$ ,  $b\ 27.5062(11)$ ,  $c\ 18.6972(9)\ \text{\AA}$ ,  $\alpha\ 140.301(3)$ ,  $\beta\ 93.033(3)$ ,  $\gamma\ 95.664(3)^\circ$ ,  
47  $V = 1720.96(14)\ \text{\AA}^3$ . The strongest lines in the X-ray powder diffraction pattern [ $d(\text{\AA})$ ]( $l$ )( $hkl$ ) are:  
48  $16.894(100)(010)$ ,  $18.204(23)(0\bar{1}1)$ ,  $4.271(9)(1\bar{4}1, 040, 120)$ ,  $11.661(8)(001)$ ,  $2.721(3)(1\bar{9}5)$ ,  
49  $4.404(3)(\bar{1}32, 1\bar{4}2)$ ,  $4.056(3)(031, 1\bar{1}2, 1\bar{5}2, \bar{1}43)$ ,  $3.891(2)(003)$ .

50 The chemical composition of veblenite from a combination of electron microprobe  
51 analysis and structural determination for  $H_2O$  and the  $Fe^{2+}/Fe^{3+}$  ratio is  $Nb_2O_5\ 11.69$ ,  $TiO_2\ 2.26$ ,  
52  $SiO_2\ 35.71$ ,  $Al_2O_3\ 0.60$ ,  $Fe_2O_3\ 10.40$ ,  $FeO\ 11.58$ ,  $MnO\ 12.84$ ,  $ZnO\ 0.36$ ,  $MgO\ 0.08$ ,  $BaO\ 1.31$ ,  
53  $SrO\ 0.09$ ,  $CaO\ 1.49$ ,  $Cs_2O\ 0.30$ ,  $K_2O\ 1.78$ ,  $Na_2O\ 0.68$ ,  $H_2O\ 4.39$ ,  $F\ 0.22$ ,  $O = F - 0.09$ , sum  
54  $95.69\text{ wt.}\%$ . The empirical formula [based on 20 (Al+Si) p.f.u.  $(K_{0.53}Ba_{0.28}Sr_{0.03}\Box_{0.16})_{\Sigma 1}$   
55  $(K_{0.72}Cs_{0.07}\Box_{1.21})_{\Sigma 2}$  $(Na_{0.72}Ca_{0.17}\Box_{1.11})_{\Sigma 2}$  $(Fe^{2+}_{5.32}Fe^{3+}_{4.13}Mn^{2+}_{5.97}Ca_{0.70}Zn_{0.15}Mg_{0.07}\Box_{0.66})_{\Sigma 17}$  $(Nb_{2.90}$   
56  $Ti_{0.93}Fe^{3+}_{0.17})_{\Sigma 4}$  $(Si_{19.61}Al_{0.39})_{\Sigma 20}$  $O_{77.01}H_{16.08}F_{0.38}$ . The simplified formula is  
57  $(K, Ba, \Box)_3(\Box, Na)_2(Fe^{2+}, Fe^{3+}, Mn^{2+})_{17}(Nb, Ti)_4(Si_2O_7)_2(Si_8O_{22})_2O_6(OH)_{10}(H_2O)_3$ . The infrared  
58 spectrum of the mineral contains the following bands ( $cm^{-1}$ ): 453, 531, 550, 654 and 958, with

59 shoulders at 1070, 1031 and 908. A broad absorption was observed between *ca* 3610 and 3300  
60 with a maximum at *ca* 3525. The crystal structure was solved by direct methods and refined to  
61 an  $R_1$  index of 9.1 %. In veblenite, the main structural unit is an HOH layer, which consists of the  
62 octahedral (O) and two heteropolyhedral (H) sheets. The H sheet is composed of  $\text{Si}_2\text{O}_7$  groups,  
63 veblenite  $\text{Si}_8\text{O}_{22}$  ribbons and Nb-dominant D octahedra. This is the first occurrence of an eight-  
64 membered  $\text{Si}_8\text{O}_{22}$  ribbon in a mineral crystal structure. In the O sheet, ( $\text{Fe}^{2+}$ ,  $\text{Fe}^{3+}$ ,  $\text{Mn}^{2+}$ )  
65 octahedra share common edges to form a modulated O sheet parallel to (001). HOH layers  
66 connect via common vertices of D octahedra and cations at the interstitial  $A(1,2)$  and  $B$  sites. In  
67 the intermediate space between two adjacent HOH layers, the  $A(1)$  site is occupied mainly by K;  
68 the  $A(2)$  site is partly occupied by K and  $\text{H}_2\text{O}$  groups, the  $B$  site is partly occupied by Na. The  
69 crystal structure of veblenite is related to several HOH structures: jinshanjiangite, niobophyllite  
70 (astrophyllite group) and nafertisite. The mineral is named in honour of David Veblen in  
71 recognition of his outstanding contributions to the field of mineralogy and crystallography.

72

73 **Keywords:** veblenite, new mineral, Seal Lake, Newfoundland and Labrador, Canada, electron-  
74 microprobe analysis, crystal structure, veblenite ribbon, nafertisite, niobophyllite, jinshanjiangite.

75

76 **Introduction**

77 During a recent work on astrophyllite-group minerals (Cámara *et al.*, 2010), the holotype sample  
78 of niobophyllite #M26148 (Royal Ontario Museum, Toronto, Canada) was studied and in that  
79 sample we observed red brown single laths included in albite. The shape suggested that these  
80 laths were a distinct phase. A test on the diffractometer on one of the longer laths (< 200 µm)  
81 gave unit-cell dimensions unknown for HOH *heterophyllosilicates* (Ferraris *et al.*, 1996; Ferraris,  
82 2008). *Heterophyllosilicates* are related to TOT silicates: in *heterophyllosilicates*, five- to six-  
83 coordinated Ti(Nb) periodically substitute a row of silicate tetrahedra in the tetrahedral (T)  
84 sheets of a TOT layer, producing a heteropolyhedral (H) sheet, while the octahedral O sheet is  
85 maintained the same. In *heterophyllosilicates*, HOH layers can link directly or contain interstitial  
86 atoms between HOH layers. A single crystal X-ray diffraction study revealed that this is a new  
87 structure type with no analogues. Here we describe the properties and the structure of this new  
88 mineral.

89 The name is in honour of David Veblen (b. 1947, Minneapolis, MN, USA) in recognition of  
90 his outstanding contributions to the fields of mineralogy and crystallography. He has established  
91 himself as one of the foremost experts of TEM in geology and has made a significant contribution  
92 to the polysomatic approach in mineralogy. The new mineral species and its name have been  
93 approved by the Commission on New Minerals, Nomenclature and Classification of the  
94 International Mineralogical Association (IMA 2010-050). The holotype specimen of veblenite (the  
95 same as that of niobophyllite) is under catalogue number #M26148 at the Royal Ontario Museum,  
96 100 Queen's Park, Toronto, Ontario M5S 2C6.

97

98 **Occurrence and associated minerals**

99 The mineral occurs at Ten Mile Lake, Seal Lake area, Newfoundland and Labrador (Canada)  
100 (latitude 54°12'N Longitude: 62°30'W). It occurs as red brown single laths and fibres included in  
101 feldspar, in a band of paragneiss consisting chiefly of albite and arfvedsonite. The geology of

102 the area has been interpreted in terms of a series of interbedded volcanic rocks and gneisses  
 103 intruded by an alkaline syenite. Associated minerals are niobophyllite, albite, arfvedsonite,  
 104 aegirine-augite, barylite, eudidymite, neptunite, Mn-rich pectolite, pyrochlore, sphalerite and  
 105 galena (Nickel *et al.*, 1964 and references therein).

106

107 **Physical and optical properties**

108 The main properties of veblenite are presented in Table 1, where they are compared to those of  
 109 jinshanjiangite, niobophyllite, and nafertisite. The mineral forms laths and fibers; laths are  
 110 hundreds of microns long and less than tens microns thick and wide (Fig. 1). Veblenite is red-  
 111 brown, with a very pale brown streak and a vitreous lustre. The mineral is translucent. It has a  
 112 perfect {001} cleavage, with splintery fracture. No parting was observed. It is not fluorescent  
 113 under 240-400 nm ultraviolet radiation. The density of the mineral and the Mohs hardness could  
 114 not be measured owing to the very small thickness of the flakes. Its calculated density (using  
 115 the empirical formula) is 3.041 g cm<sup>-3</sup>. The mineral is biaxial negative with  $\alpha$  1.676,  $\beta$  1.688,  $\gamma$   
 116 1.692 ( $\lambda$  590 nm), all  $\pm$  0.002,  $2V(\text{meas.}) = 65.3(1.2)^\circ$ ,  $2V(\text{calc.}) = 59.6^\circ$ , with no determined  
 117 dispersion. Optical orientation is

	<b>a</b>	<b>b</b>	<b>c</b>
118			
119	X	87.8°	92.3° 126.7°
120	Y	96.0°	168.2° 36.9°
121	Z	173.6°	78.5° 93.0°

122 It is pleochroic with X = black, Y = black, Z = orange-brown. A Gladston-Dale compatibility index  
 123 of 0.025 is rated as excellent.

124 The infrared powder absorption spectrum was recorded with a Nicolet FTIR 740  
 125 spectrophotometer in the range 4000-400 cm<sup>-1</sup> (Fig. 2). In the principal OH-stretching region  
 126 (3800-3000 cm<sup>-1</sup>), the spectrum shows a broad absorption between ~3610 and ~3300 cm<sup>-1</sup> with  
 127 a maximum at ~3525 cm<sup>-1</sup> in accord with the presence of several OH and H<sub>2</sub>O groups in the

128 structure. Several weak bands between 3000 and 2000  $\text{cm}^{-1}$  and weak bands at 1480 and 1377  
129  $\text{cm}^{-1}$  are due to glue that was used during transport of the crystals and subsequently could not  
130 be completely removed from the very delicate crystals. There is a band at 1637  $\text{cm}^{-1}$  due to the  
131 H-O-H bend of  $\text{H}_2\text{O}$  groups in the structure. There is a sharp intense band at 958 with shoulders  
132 at 1070, 1031 and 908  $\text{cm}^{-1}$  due to the various stretching modes of the  $\text{SiO}_4$  group, and weaker  
133 bands at 654, 550, 531 and 453  $\text{cm}^{-1}$  due to complex lattice modes involving the octahedra and  
134 coupled motions between the various polyhedra.

135

### 136 **Chemical composition**

137 The chemical composition of veblenite was determined with a Cameca SX-100 electron-  
138 microprobe in wavelength-dispersion mode with an accelerating voltage of 15 kV, a specimen  
139 current of 20 nA, a beam size of 10  $\mu\text{m}$  and count times on peak and background of 20 and 10  
140 s, respectively. The following standards were used:  $\text{Ba}_2\text{NaNb}_5\text{O}_{15}$  (Ba, Nb),  $\text{SrTiO}_3$  (Sr), titanite  
141 (Ti), diopside (Si, Ca), andalusite (Al), fayalite (Fe), spessartine (Mn), forsterite (Mg), gahnite  
142 (Zn) orthoclase (K), albite (Na), pollucite (Cs) and F-bearing riebeckite (F). Sn, Zr, Ta, Pb and  
143 Rb were sought but not detected; Li and Be were sought by LA-ICP-MS but not detected. Data  
144 were reduced using the PAP procedure of Pouchou and Pichoir (1985).  $\text{H}_2\text{O}$  and the  $\text{Fe}^{3+}/\text{Fe}^{2+}$   
145 ratio were calculated from structure refinement. The low total of ~91 wt% is due to the thinness  
146 of the crystal. We did not have material sufficient for direct determination of  $\text{H}_2\text{O}$ , but the  
147 presence of  $\text{H}_2\text{O}$  was confirmed by infrared spectroscopy (see above). The chemical  
148 composition of veblenite is given in Table 2. The empirical formula (based on Si + Al = 20 atoms  
149 p.f.u.) is  $(\text{K}_{0.53}\text{Ba}_{0.28}\text{Sr}_{0.03}\square_{0.16})_{\Sigma 1}(\text{K}_{0.72}\text{Cs}_{0.07}\square_{1.21})_{\Sigma 2}(\text{Na}_{0.72}\text{Ca}_{0.17}\square_{1.11})_{\Sigma 2}$   
150  $(\text{Fe}^{2+}_{5.32}\text{Fe}^{3+}_{4.13}\text{Mn}^{2+}_{5.97}\text{Ca}_{0.70}\text{Zn}_{0.15}\text{Mg}_{0.07}\square_{0.66})_{\Sigma 17}(\text{Nb}_{2.90}\text{Ti}_{0.93}\text{Fe}^{3+}_{0.17})_{\Sigma 4}(\text{Si}_{19.61}\text{Al}_{0.39})_{\Sigma 20}\text{O}_{77.01}\text{H}_{16.08}$   
151  $\text{F}_{0.38}$ ,  $Z = 1$ .

152

153

## 154 **X-ray powder diffraction**

155 The powder-diffraction pattern for veblenite was recorded **at the Canadian Museum of Nature**  
156 using a Bruker D8 Discover micro-powder diffractometer with a Hi-Star multi-wire 2D detector at  
157 **12 cm, calibrated following Rowe (2009) and using a psudogandolfi approach.** Table 3 shows  
158 the X-ray powder-diffraction data (for  $\text{CuK}\alpha$ ,  $\lambda = 1.54178 \text{ \AA}$ ; 40 kV / 40 mA) with refined unit-cell  
159 dimensions; the latter are in close agreement with corresponding values determined by single-  
160 crystal diffraction (Table 4).

161

## 162 **Crystal structure**

### 163 *X-ray data collection and structure refinement*

164 X-ray diffraction data for the single crystal of veblenite were collected with a Bruker *P4*  
165 diffractometer with a CCD 4K Smart detector ( $\text{MoK}\alpha$  radiation) **using the largest crystal found in**  
166 **the sample included in a feldspar grain, extracted using a razor blade to open the grain; the**  
167 **crystal came off nicely clean or matrix (no additional spots were observed in the diffraction**  
168 **images).** The intensities of 25883 reflections using  $0.2^\circ$  frame and an integration time of 60 s, of  
169 which 15845 are unique ( $R_{\text{int}} = 9.47\%$ ). An empirical absorption correction (SADABS, Sheldrick,  
170 2008) was applied. Only reflections with  $-5 < h < 5$ ,  $-30 < k < 30$ ,  $-20 < l < 20$ , i.e.,  $46^\circ 2\theta$ ,  
171 corresponding to 4777 unique reflections  $R_{\text{int}} = 6.66\%$  were used for refinement. The refined  
172 unit-cell parameters were obtained from 7614 reflections with  $I > 10\sigma I$  (Table 4). The crystal  
173 structure of veblenite was solved in space group  $P\bar{1}$  by direct methods using SHELXS  
174 (Sheldrick, 2008) and refined with the Bruker SHELXTL Version 5.1 system of programs  
175 (Sheldrick, 2008). The crystal structure contains 3 groups of cation sites: *D* and *Si* sites of the H  
176 sheet, *M* sites of the O sheet, and interstitial *A* and *B* sites; site labeling is in accord with TS-  
177 block minerals (Sokolova, 2006) and astrophyllite-group minerals (Sokolova, 2012). Because of  
178 the small size of the single crystal, it was not possible to collect enough reflections for a full



179 anisotropic refinement. Therefore displacement parameters were refined anisotropically only for  
180 atoms of the O sheet, D and Si atoms of H sheets, and interstitial atoms. The occupancies of  
181 cations at the  $M(1)$ - $M(6)$  sites were fixed (scattering curve of Fe) while those at the  $D(1A)$ - $D(2B)$   
182 and  $M(7)$ - $M(9)$  sites were refined. The observed scattering at the  $M(7)$ - $M(9)$  sites was held fixed  
183 in the last cycles of refinement (scattering curve of Mn). Occupancies of atoms were also  
184 refined for the interstitial  $A(1)$  site (scattering curve of Ba),  $A(2A)$ - $A(2D)$  sites (scattering curve of  
185 K),  $B$  site (scattering curve of Na), and for anion sites [ $W(1)$ - $W(5)$ ], corresponding to interstitial  
186  $H_2O$  groups, with  $U_{iso}$  fixed at  $0.05 \text{ \AA}^2$ . The structure model was refined to an  $R_1$  value of 9.05%.

187         At the last stages of the refinement, 3 peaks with magnitudes of ca. 1.5 e/ were found as  
188 satellites of the  $M(1)$ ,  $M(6)$  and  $M(9)$  sites. Occupancies of atoms at these subsidiary peaks  
189 were refined with the scattering curves of Fe, Fe and Mn, respectively, and with  $U_{iso}$  fixed at  
190  $0.01 \text{ \AA}^2$ . Refined occupancies of these subsidiary peaks vary from 2 to 5 %. Scattering curves  
191 for neutral atoms were taken from International Tables for Crystallography (Wilson, 1992). The  
192 unusual cell setting chosen for the structure (Tables 1, 3 and 4) is obtained from the reduced  
193 cell  $a = 5.3761(3)$ ,  $b = 17.7419(10)$ ,  $c = 18.6972(11) \text{ \AA}$ ,  $\alpha = 97.991(1)$ ,  $\beta = 93.032(2)$ ,  $\gamma =$   
194  $102.050(1)^\circ$  via the transformation  $(1,0,0|0,1,-1|0,0,1)$ . The chosen setting with a large  $\alpha$  is  
195 preferred in order to compare the structure topology of veblenite to those of jinshajiangite and  
196 niobophyllite. Details of data collection and structure refinement are given in Table 4, final atom  
197 parameters are given in Table 5, selected interatomic distances in Table 6, refined site-  
198 scattering values and assigned populations for selected cation sites are given in Table 7, and  
199 bond valences in Table 8 (bond-valence parameters from Brown, 1981). Tables of structure  
200 factors and anisotropic displacement parameters for several atoms have been deposited with  
201 the Principal Editor of *Mineralogical Magazine* and are available from  
202 [www.minersoc.org/pages/e\\_journals/dep\\_mat.html](http://www.minersoc.org/pages/e_journals/dep_mat.html).

203

204 *Site-population assignment*

205 As we did not have enough material to determine the  $\text{Fe}^{3+}/\text{Fe}^{2+}$  ratio directly by Mössbauer  
206 spectroscopy, the  $\text{Fe}^{3+}/\text{Fe}^{2+}$  ratio was calculated from the M-O distances of the M(1-9)  
207 octahedra of the O sheet; minor  $\text{Fe}^{3+}$  was added to fill (Nb,Ti)-dominant *D* sites. Consider first  
208 the two (Nb,Ti)-dominant *D*(1,2) sites in the H sheet. Each *D* site is split in two sites: *D*(1A) and  
209 *D*(1B), and *D*(2A) and *D*(2B). We assign cations to these sites assuming 50% occupancy for  
210 each split site. The split site is related to a different charge arrangement: *D*(1A) and *D*(2B) sites  
211 are closer to the O sheet and have a lower charge, while *D*(1B) and *D*(2A) sites are further from  
212 the O sheet and are almost fully occupied by Nb. Total Nb + Ti is < 4 a.p.f.u. Thus we assign  
213  $\text{Fe}^{3+}$  to achieve 100%-occupancy of the *D* sites. The resulting calculated site-scattering is  
214 significantly lower than the aggregate refined scattering at these sites (141.19 versus 153.42  
215 e.p.f.u., Table 7), indicating heavier atom composition, although the chemical analyses  
216 confirmed the absence of Sn and Ta. We assign Si with minor Al to ten tetrahedral *Si* sites, with  
217  $\langle \text{Si-O} \rangle = 1.615 \text{ \AA}$ .

218 Consider next the octahedral sites in the O sheet. There are nine independent [6]-  
219 coordinated *M* sites [*M*(1-9)], with size of a corresponding octahedron increasing from *M*(1) to  
220 *M*(9); the *M*(1-9) sites can accommodate up to 17 a.p.f.u. Site scattering for the *M* sites varies  
221 from 20 to 26 electrons per site (e.p.s.), with the lowest values observed at the *M*(7-9) sites.  
222 Total refined scattering at the *M* sites is 413.5 e.p.f.u., which agrees well with the calculated  
223 site-scattering from the remaining  $\text{Fe}^{3+}$  plus ( $\text{Fe}^{2+} + \text{Mn}^{2+} + \text{Ca} + \text{Zn} + \text{Mg}$ ), with a vacancy of  
224 0.66 p.f.u. On the basis of observed bond distances and incident bond-valence at these sites  
225 (Table 8), we assign 2/3 of  $\text{Fe}^{3+}$  and 1/3 of  $\text{Fe}^{2+}$  to each *M*(1), *M*(2) and *M*(3) site (see above)  
226 (Table 7). We allocate the remaining  $\text{Fe}^{3+}$  equally to the *M*(4) and *M*(5) sites, plus an equal  
227 quantity of  $\text{Mn}^{2+}$  to account for the larger size of these two octahedra. The *M*(6) octahedron is  
228 larger and we assign the remaining  $\text{Fe}^{2+}$  and  $\text{Mn}^{2+}$ . The larger *M*(7)-*M*(9) sites give different  
229 refined scattering values, being higher for the *M*(8) site, with the *M*(8) octahedron being slightly  
230 smaller than the *M*(7,9) octahedra. Therefore we assign all the Zn + Mg to the *M*(8) site, while

231 Ca is distributed equally among the  $M(7)$  and  $M(9)$  sites, leaving a 15% vacancy at the latter two  
232 sites in agreement with the refined site-scattering at these sites (Table 7). Thus we have three  
233  $\text{Fe}^{3+}$ -dominant  $M(1,2,3)$  sites [ $\langle M-\varphi \rangle = 2.06 \text{ \AA}$  (where  $\varphi = \text{O, OH}$ )]; three  $\text{Fe}^{2+}$ -dominant  $M(4,5,6)$   
234 sites [ $\langle M-\varphi \rangle = 2.14 \text{ \AA}$ ] and three  $\text{Mn}^{2+}$ -dominant  $M(7,8,9)$  sites [ $\langle M-\varphi \rangle = 2.21 \text{ \AA}$ ].

235 Consider the interstitial  $A(1,2)$  and  $B$  sites, with refined site-scattering values of 26.89,  
236 17.53 and 11.32 e.p.f.u., respectively (Table 7). The cations to be assigned to these sites are  
237 Na, Ba, Sr, K and Cs, with a total scattering of 55.74 e.p.f.u. (Table 7).  $A(2)$  is split into four  
238 sites:  $A(2A)$ ,  $A(2B)$ ,  $A(2C)$  and  $A(2D)$ . The  $A(1)$  and  $A(2A-2D)$  polyhedra are larger (mean bond  
239 distances of 3.17 and 3.26  $\text{\AA}$ , respectively), while the  $B$  polyhedron is smaller, with  $\langle B-\varphi \rangle = 2.72$   
240  $\text{\AA}$ , and  $B$  has lower scattering than the  $A$  sites. Therefore, we allocate all the available Na as  
241 well as the remaining Ca to the  $B$  site, which yields 11.32 e.p.f.u. in good agreement with the  
242 refined value of 11.3(4) e.p.f.u. Vacancy is therefore dominant at the  $B$  site (Table 7). The  
243 higher refined scattering at the  $A(1)$  site forces us to assign all the Ba + Sr from the analysis to  
244 that site. Cs is the largest cation left to be assigned and we consequently allocate it to the  $A(2A-$   
245  $2D)$  sites. The remaining K was distributed so that the best agreement with the refined site-  
246 scattering was obtained (Table 7). The  $A(1)$  site is K dominant, while the  $A(2)$  sites are vacancy  
247 dominant.

248

### 249 **General topology of the crystal structure**

250 The crystal structure of veblenite consists of HOH layers stacked along  $\mathbf{c}$  (Fig. 3): two H sheets  
251 and an O sheet constitute an HOH layer, with a new topology that has not been found in any  
252 other HOH structures. M octahedra share common edges to form a modulated trioctahedral  
253 close-packed (O) sheet parallel to (001) (Fig. 3). The H sheet is composed of  $\text{Si}_2\text{O}_7$  groups,  
254  $\text{Si}_8\text{O}_{22}$  ribbons and [6]-coordinated Nb-dominant D octahedra (Fig. 4b). Two H sheets of the  
255 HOH layer are identical. This is the first occurrence of a  $\text{Si}_8\text{O}_{22}$  ribbon in a mineral structure, and  
256 we call it the *veblenite* ribbon. This is also the first occurrence of the H sheets of the

257 composition  $[\text{Nb}_3\text{Ti}(\text{Si}_2\text{O}_7)_2(\text{Si}_8\text{O}_{22})_2]^{15-}$ . H sheets link to the central O sheet via common anions  
258 of M octahedra and Si and D polyhedra. The  $t_1$  repeat of  $\sim 5.5 \text{ \AA}$  is common to Ti-disilicates  
259 (Sokolova, 2006) and astrophyllite-group minerals (Sokolova, 2012). The HOH layers are  
260 stacked along [001] and show a lateral shift along [010], which allows linkage via common  
261 anions of D polyhedra of the H sheets. This type of linkage yields two types of channels running  
262 along [100]: wide and narrow channels that alternate in both [010] and [001] directions (Fig. 5a).  
263 Along [100], interstitial *B* sites are partly occupied by Na (Fig. 5a). Within the narrow [100]  
264 channels, *A*(1) interstitial sites are almost fully occupied by K (Fig. 5a), while at the narrower  
265 sides of the wide [001] channels, there are interstitial K cations in partially occupied *A*(2A-D)  
266 split positions. In the central part of the wide channels,  $\text{H}_2\text{O}$  groups coordinate K at the *A*(2)  
267 sites (Fig. 5a).

268 The crystal structure of veblenite is closely related to the structure of nafertisite, ideally  
269  $(\text{Na},\text{K})_2(\text{Fe}^{2+},\text{Fe}^{3+},\square)_{10}[\text{Ti}_2(\text{Si},\text{Fe}^{3+},\text{Al})_{12}\text{O}_{37}](\text{OH},\text{O})_6$  (Ferraris *et al.*, 1996), niobophyllite, ideally  
270  $\text{K}_2\text{NaFe}^{2+}_7(\text{Nb},\text{Ti})_2(\text{Si}_4\text{O}_{12})_2\text{O}_2(\text{OH})_4(\text{O},\text{OH})$  (Cámara *et al.*, 2010), an astrophyllite-group mineral,  
271 and jinshaijangite, ideally  $\text{NaBaFe}^{2+}_4\text{Ti}_2(\text{Si}_2\text{O}_7)_2\text{O}_2(\text{OH})_2\text{F}$  (Sokolova *et al.*, 2009), a TS-block  
272 mineral of Group II (Sokolova, 2006). The topology of the veblenite structure was generated by  
273 Hawthorne (2012) who used a structure-generating function for polysomatic TOT and HOH  
274 structures.

275

## 276 **Description of cation and anion sites**

### 277 *Cation sites*

278 The crystal structure contains 3 groups of cation sites: *D* and *Si* sites of the H sheet, *M* sites of  
279 the O sheet, and interstitial *A* and *B* sites (see above).

280

### 281 *O sheet*

282 There are nine cation sites in the O sheet: the Fe<sup>3+</sup>-dominant *M*(1,2,3) sites, the Fe<sup>2+</sup>-  
 283 dominant *M*(4,5,6) sites and Mn<sup>2+</sup>-dominant *M*(7,8,9) sites (Fig. 4a). Fe<sup>3+</sup> occurs only at  
 284 the *M*(1-6) sites and vacancies are present at the *M*(7,8,9) sites. The *M*(1,2,3) sites are  
 285 occupied by 2/3 Fe<sup>3+</sup> and 1/3 Fe<sup>2+</sup> with  $\langle M(1,2,3)-\varphi \rangle = 2.06 \text{ \AA}$  ( $\varphi$  = unspecified anion),  
 286 and are coordinated by four O atoms shared with Si atoms and two monovalent X<sup>O<sub>A</sub></sup>  
 287 anions (see section on *Anion sites* below) (Tables 6 and 7). The *M*(4,5) sites are  
 288 occupied by 0.62 Fe<sup>2+</sup> a.p.s., 0.19 a.p.s. Fe<sup>3+</sup> and 0.19 Mn<sup>2+</sup> a.p.f. with  $\langle M(4,5)-\varphi \rangle =$   
 289 2.13 Å, and are coordinated by three O atoms shared with Si atoms, one O atom at the  
 290 X<sup>O<sub>D</sub></sup> site (shared with a *D* atom), and two monovalent X<sup>O<sub>A</sub></sup> anions (Tables 6, 7 and 8).  
 291 The *M*(6) site is occupied only by divalent cations (0.61 a.p.s. Fe<sup>2+</sup> and 0.19 a.p.f. Mn<sup>2+</sup>)  
 292 with a  $\langle M(6)-\varphi \rangle$  distance of 2.15 Å and, like the *M*(4,5) sites, it is coordinated by three O  
 293 atoms shared with Si atoms, one X<sup>O<sub>D</sub></sup> divalent anion occupied by oxygen, and two  
 294 monovalent X<sup>O<sub>A</sub></sup> anions (Tables 6, 7 and 8) The *M*(7,9) sites are occupied by 0.67 a.p.s.  
 295 Mn<sup>2+</sup>, 0.18 a.p.s. Ca and 0.15 vacancy and are coordinated by four O atoms shared with  
 296 Si atoms, one X<sup>O<sub>D</sub></sup> divalent anion occupied by oxygen, and one monovalent X<sup>O<sub>A</sub></sup> anion,  
 297 with a  $\langle M(7,9)-\varphi \rangle$  distance of 2.22 Å, while the *M*(8) site is occupied by 0.86 a.p.s. Mn<sup>2+</sup>,  
 298 0.08 a.p.s. Zn and 0.03 a.p.s. Mg and 0.03 vacancy per site and is coordinated by three  
 299 O atoms shared with Si atoms, one X<sup>O<sub>D</sub></sup> divalent anion occupied by oxygen, and two  
 300 monovalent X<sup>O<sub>A</sub></sup> anions, with  $\langle M(8)-\varphi \rangle = 2.19 \text{ \AA}$  (Tables 6, 7 and 8). Cations of the O  
 301 sheet sum to (Fe<sup>2+</sup><sub>5.32</sub>Fe<sup>3+</sup><sub>4.13</sub>Mn<sup>2+</sup><sub>5.97</sub>Ca<sub>0.70</sub>Zn<sub>0.15</sub>Mg<sub>0.07</sub>□<sub>0.66</sub>) a.p.f.u. (Table 7), with ideal  
 302 and simplified compositions of (Fe<sup>2+</sup><sub>5</sub>Fe<sup>3+</sup><sub>4</sub>Mn<sup>2+</sup><sub>7</sub>□) and (Fe<sup>2+</sup>,Fe<sup>3+</sup>,Mn<sup>2+</sup>)<sub>17</sub> a.p.f.u.,  
 303 respectively.

304

### 305 *H sheets*

306 In the H sheets, there are ten tetrahedrally coordinated sites occupied by Si with a  $\langle \text{Si-}$   
 307 O  $\rangle$  distance of 1.615 Å (Table 6, Fig. 4b, c). The longest Si-O distance is usually the one

308 to the O atom shared with the M atoms in the O sheet. There are two Si tetrahedra that  
309 are slightly larger [*Si*(2) and *Si*(8), with  $\langle \text{Si-O} \rangle = 1.63 \text{ \AA}$ ] and the *Si*(2,8) sites may  
310 therefore host up to 10 % Al. Interestingly, the *Si*(2,8) tetrahedra share an oxygen atom  
311 with two Mn<sup>2+</sup>-dominant M(7,8) octahedra; i.e., two of the largest ones] and a Fe<sup>3+</sup>-  
312 dominant M(3) octahedron], while all other Si tetrahedra share an apex with one Fe<sup>2+</sup>-  
313 dominant, one Mn<sup>2+</sup>-dominant and one Fe<sup>3+</sup>-dominant octahedra, and would nominally  
314 have less incident bond-valence. In fact, these two tetrahedral sites have the lowest  
315 incident bond-valence sums among all the *Si* sites (Table 8). Sokolova (2012) showed  
316 that Si<sub>2</sub>O<sub>7</sub> groups of the astrophyllite [Si<sub>4</sub>O<sub>12</sub>] ribbon have a very restricted range of Si-O-  
317 Si angles, i.e., 138-143°, compared to the Si<sub>2</sub>O<sub>7</sub> groups in the Ti-silicate minerals, which  
318 show a wider range of Si-O-Si angles: ~134 to ~206° (Sokolova, 2006). The Si-O-Si  
319 angles in veblenite range from 138 to 143° (Table 6) as in the astrophyllite-group  
320 structures, indicating reduced flexibility of the tetrahedral ribbons to match connectivity  
321 with the O sheet.

322 There are two [6]-coordinated *D*(1,2) sites that each split into two sites: *D*(1A, 1B)  
323 and *D*(2A, 2B). Each of the latter four sites is octahedrally coordinated by six O atoms,  
324 with  $\langle \text{D-O} \rangle = 1.98 \text{ \AA}$  (Table 6). There are three Nb-dominant sites: *D*(1A,1B, 2A) and  
325 one Ti-dominant *D*(2B) site, with total Nb<sub>2.90</sub>Ti<sub>0.93</sub>Fe<sup>3+</sup><sub>0.17</sub>, ideally Nb<sub>3</sub>Ti a.p.f.u. (Table 7).  
326 In veblenite, D octahedra of adjacent HOH layers connect via a bridge oxygen at the X<sup>P</sup><sub>D</sub>  
327 site (Fig. 3). Four of six O atoms coordinating each D atom are common to a D  
328 octahedron and four Si tetrahedra; one atom is common to a D octahedron and three M  
329 octahedra of the O sheet. The X<sup>O</sup><sub>D</sub>(1) atom belongs to the *D*(1A,1B) octahedra and the  
330 X<sup>O</sup><sub>D</sub>(2) atom belongs to the *D*(2A,2B) octahedra, and the sixth O atom occurs at the X<sup>P</sup><sub>D</sub>  
331 site. The shortest and the longest D-X<sup>O</sup><sub>M</sub> distances are 1.86 Å and 2.23 Å, respectively,  
332 while the shortest and the longest D-X<sup>P</sup><sub>D</sub> distances are 1.79 Å and 2.15 Å, respectively  
333 (Fig. 6). These distances are within the observed distances for Nb and Ti at the M<sup>H</sup> sites

334 in the H sheet in Ti-disilicates: e.g., epistolite (Sokolova and Hawthorne, 2004),  
335 vuonnemite (Ercit *et al.*, 1998), bornemanite (Cámara and Sokolova, 2007),  
336 nechelyustovite (Cámara and Sokolova, 2009) and kazanskyite (Cámara *et al.*, 2012).

337 However we are left with a question: which two of four D(1A-2B) sites can form  
338 the D- $X_D^P$ -D bridges. To do this, we must consider SRO (Short-range order)  
339 arrangements.

340 *Short-range order arrangements of the D sites.* The  $X_D^P$  atom receives bond-  
341 valence contributions from atoms at four *D* and two *B* sites occupied at 50% mainly by  
342 Nb and Na (contributions from the *A*(2) site occupied by K at ca. 40% are too small and  
343 not considered here) (Table 7). Note that D(1A)-D(1B) and D(2A)-D(2B) occur at short  
344 distances of  $\sim 0.33$  Å and cannot be locally occupied. Hence, in the structure, the  $X_D^P$  site  
345 is [4] coordinated by two *D* sites and two *B* sites. The incident bond-valence of 1.92 vu  
346 (valence units) at the  $X_D^P$  atom (Table 8) tell us that the  $X_D^P$  site is occupied by an O  
347 atom both in a long-range structure and short-range-order arrangements. Consider the  
348 short-range-ordered arrangement where all cation sites (*D* and *B*) are fully occupied, i.e.,  
349 at 100%. To calculate the bond-valence contributions to the  $X_D^P$  atom from *D* and *B*  
350 atoms, we must multiply their bond-valence contributions by 2 (corresponding to 50%-  
351 occupancy): 0.24 x 2 = 0.48 vu [D(1A)], 1.34 vu [D(1B)], 1.30 vu [D(2A)], 0.48 vu [D(2B)]  
352 and 0.24 vu (*B* x 2). Contributions from D(1A), D(2B) and 2 *B* atoms sum to 1.20 vu  
353 which is too low for an O atom. Contributions from the D(1B), D(2A) and 2*B* atoms sum  
354 to 2.88 vu which is too high for an O atom. We are left with two possible short-range-  
355 ordered arrangements: contributions from (1) [D(1A), D(2A) and 2*B*] and (2) [D(1B),  
356 D(2B) and 2*B*] atoms sum to 2.02 and 2.06 vu, respectively, compensating the 2<sup>-</sup> charge  
357 of an O atom at the  $X_D^P$  site. Hence two types of D- $X_D^P$ -D bridges can occur in the  
358 structure: (SRO-1) D(1A)-O-D(2A) and (SRO-2) D(1B)-O-D(2B) (Fig. 6). Possible  
359 occurrence of these two short-range-ordered arrangements explains the difference in D-

360  $X_D^P$  and  $D-X_D^O$  distances. For SRO-1, D(1A)-O-D(2A), the  $X_D^P$  anion receives a larger  
361 bond-valence contribution from D(2A) (1.30 vu, shorter distance of 1.81 Å) and needs a  
362 smaller contribution from D(1A) (0.4 vu, longer distance of 2.14 Å). Note that the longer  
363 D(1A)- $X_D^P$  distance of 2.14 Å corresponds to the shorter D(1A)- $X_D^O(1)$  distance of 1.88 Å  
364 [cf. D(2A)- $X_D^P$  = 1.81 Å versus D(2A)- $X_D^O(2)$  = 2.20 Å] (Fig. 6). It seems that the order of  
365 M cations in the O sheet forces the D atoms to change their positions in order to satisfy  
366 the bond-valence requirements at the  $X_D^O$  anions.

367 The D cations of two H sheets sum to  $Nb_{2.90}Ti_{0.93}Fe^{3+}_{0.17}$  a.p.f.u. (Table 7), with  
368 ideal and simplified compositions of  $Nb_3Ti$  and  $(Nb,Ti)_4$  a.p.f.u., respectively. We will  
369 consider the Si atoms as part of the complex oxyanions (see below).

370

### 371 *Interstitial sites*

372 In veblenite, there are two interstitial sites: *A* and *B*. There are two *A* sites: *A*(1) in the  
373 narrow channel and *A*(2) in the wider channel (Fig. 5a). The *A*(1) site is [12]-coordinated  
374 by the basal oxygen atoms of Si tetrahedra on both sides of the channel. It is almost fully  
375 occupied by 0.53 a.p.s. K, 0.28 a.p.s. Ba and 0.03 a.p.s. Sr and with 0.16 □ per site,  
376 and  $\langle A(1)-\phi \rangle = 3.17$  Å (Table 6). We write the ideal and simplified compositions of the  
377 *A*(1) site as K and (K,Ba), respectively. The *A*(2) site is split in 4 mutually exclusive  
378 positions with partial occupancy (Table 7), being dominantly vacant (Fig. 5b). These split  
379 positions are [9-10]-coordinated by oxygen from the basal planes of tetrahedra of the  
380 adjacent H layers and by H<sub>2</sub>O groups at partly occupied *W* sites (see section on *Anion*  
381 *sites* below), with  $\langle A(2A,B)-\phi \rangle = 3.19$  Å,  $\langle A(2C)-\phi \rangle = 3.12$  Å, and  $\langle A(2D)-\phi \rangle = 3.26$  Å.  
382 Aggregate composition for the *A*(2A-2D) sites is 0.60 □ p.s. + 0.36 a.p.s. K, and 0.04  
383 a.p.s. Cs. We write the ideal and simplified compositions of the *A*(2) site as (□K) and  
384 (□,K)<sub>2</sub>, respectively. The occupancy of *A*(2) sites is probably related to the Nb<sub>1</sub>Ti  
385 substitution at the adjacent D sites. Therefore, the *A*(2) composition is constrained by



386 the relation  $A(2)_n = Nb_{4-n}Ti_n$ , although the  $Nb_{-1}Ti$  substitution could be compensated also  
387 by increasing the amount of  $Fe^{3+}$  at the  $M(1-3)$  sites.

388 The  $B$  site occurs between four  $D$  sites (from adjacent HOH layers, Figs. 5a, b);  
389 they are [10]-coordinated by the basal oxygen atoms of the Si tetrahedra of the adjacent  
390 HOH layers and by the oxygen atom shared by two  $D$  atoms from different HOH layers,  
391 with  $\langle B-O \rangle = 2.72 \text{ \AA}$ . The  $B$  site is occupied at 45% by 0.36 a.p.s. Na and 0.09 a.p.s. Ca  
392 (Table 7). We write the ideal and simplified compositions of the  $B$  site as  $(\square Na)$  and  
393  $(\square, Na)$ , respectively, and the ideal and simplified compositions of the interstitial  
394  $A(1)A(2)B$  sites are  $K(\square K)(\square Na) = K_2\square_2Na$  and  $(K, Ba)(\square, K)_2(\square, Na)_2$ , respectively.

395  
396 We write the cation part of the ideal and simplified formulas the sum of the  $M$  sites of the

397 O sheet +  $D$  sites of two H sheets + interstitial  $A$  and  $B$  sites: (1) ideal formula:

398  $(Fe^{2+}_5Fe^{3+}_4Mn^{2+}_7\square) + Nb_3Ti + K(\square K)(\square Na) = K_2\square_2Na(Fe^{2+}_5Fe^{3+}_4Mn^{2+}_7\square)Nb_3Ti$ , with a total  
399 charge of  $58^+$ ; (2) simplified formula:  $(Fe^{2+}, Fe^{3+}, Mn^{2+})_{17} + (Nb, Ti)_4 + (K, Ba)(\square, K)_2(\square, Na)_2 =$   
400  $[(K, Ba, \square)_3(\square, Na)_2(Fe^{2+}, Fe^{3+}, Mn^{2+})_{17}(Nb, Ti)_4]$  a.p.f.u.

401

#### 402 *Anion sites*

403 Following the nomenclature of the anion sites by Sokolova (2012), we label the X anions:  $2 X^O_D$   
404 = anions at common vertices of 3 M and D polyhedra;  $5 X^O_A$  = monovalent anions at common  
405 vertices of 3 M polyhedra;  $X^P_D$  = apical anion shared by two D cations from two different HOH  
406 layers. Additionally, there are 5 interstitial  $H_2O$  groups (with partial occupancy) which we label  
407  $W(1-5)$ .

408 There are 29 anion sites, O(1-29), occupied by O atoms which form the tetrahedral  
409 coordination of the Si atoms (Tables 5, 6). Si(1-8) and O(1-29) atoms form two distinct complex  
410 oxyanions,  $(Si_2O_7)_2$  and  $(Si_8O_{22})_2$  per formula unit. There are two sites,  $X^O_D(1,2)$ , which are  
411 common anions for the D polyhedra and three octahedra of the O sheet (Tables 5, 6) and give

412 O<sub>4</sub> p.f.u. These anions receive bond valences of 1.71-1.74 vu (Table 8) and hence are O atoms.  
 413 The low incident bond-valence is probably due to the split of the *D* sites. There is one anion,  
 414 X<sup>P</sup><sub>D</sub>, shared by two *D* atoms of adjacent HOH layers; this anion receives a bond valence of 1.92  
 415 vu (Table 8) and hence is an O atom. The X<sup>P</sup><sub>D</sub> site gives O<sub>2</sub> p.f.u. There are five X<sup>O</sup><sub>A(1-5)</sub> sites  
 416 that are common anions for three octahedra of the O sheet. They receive bond valences of  
 417 1.20-1.38 vu (Table 8), and hence are monovalent anions (OH or F). The chemical analysis  
 418 gives F 0.38 a.p.f.u. and we need 10 – 0.38 = 9.62 OH p.f.u. to fill these five sites. Therefore,  
 419 we assign OH<sub>9.62</sub>F<sub>0.38</sub> to the five X<sup>O</sup><sub>A(1-5)</sub> sites. Ideally, the five X<sup>O</sup><sub>A</sub> sites give (OH)<sub>10</sub> p.f.u. There  
 420 are H<sub>2</sub>O groups at the five *W*(1-5) sites, and the O atoms of the H<sub>2</sub>O groups are bonded to the  
 421 A(2A-D) cations. The *W*(1-5) sites are partly occupied (Table 5): *W*(1) and *W*(2) at 57 and 43%,  
 422 and *W*(3,4,5) at 23, 17 and 21%, respectively. Local occupancy of both *W*(1) and *W*(2) is  
 423 incompatible as *W*(1)-*W*(2) = 2.59(5) Å. Each H<sub>2</sub>O group at one of these two sites bonds weakly  
 424 to the basal oxygen atoms of the tetrahedra in the Si<sub>8</sub>O<sub>22</sub> ribbon. Occupancy of the *W*(3) site  
 425 cannot be locally associated with occupancy of the *W*(4) and *W*(5) sites as *W*(3)-*W*(5) =  
 426 1.11(12) Å and *W*(3)-*W*(5) = 2.06(15) Å. The occupancy of the *W*(3-5) sites is linked to the  
 427 occupancy of the A(2A-2D) sites. The observed occupancy of the *W*(3-5) is lower than that at  
 428 the A(2A-2D) sites, probably due to the difficulty in correctly calculating the scattering at split  
 429 positions with data from such a thin crystal. In veblenite, the *W*(1,2) and *W*(3-5) sites give  
 430 (H<sub>2</sub>O)<sub>2</sub> and [(H<sub>2</sub>O)<sub>1.23</sub>□<sub>2.77</sub>] p.f.u., respectively, ideally (H<sub>2</sub>O)<sub>3</sub> p.f.u.

431 To conclude, we write the anion part of the ideal structural formula as the sum of the  
 432 complex anions and the simple anions (charge is given in brackets): (Si<sub>2</sub>O<sub>7</sub>)<sub>2</sub> (12<sup>-</sup>) + (Si<sub>8</sub>O<sub>22</sub>)<sub>2</sub>  
 433 (24<sup>-</sup>) + O<sub>4</sub> [X<sup>O</sup><sub>D(1,2)</sub>] (8<sup>-</sup>) + O<sub>2</sub> [X<sup>P</sup><sub>D</sub>] (4<sup>-</sup>) + (OH)<sub>10</sub> [X<sup>O</sup><sub>A(1-5)</sub>] (10<sup>-</sup>) + (H<sub>2</sub>O)<sub>3</sub> [*W*(1-5)] =  
 434 (Si<sub>2</sub>O<sub>7</sub>)<sub>2</sub>(Si<sub>8</sub>O<sub>22</sub>)<sub>2</sub>O<sub>6</sub>(OH)<sub>10</sub>(H<sub>2</sub>O)<sub>3</sub>, with a total charge of 58<sup>-</sup>.

435 Based on the SREF results and bond-valence calculations, we write the ideal and  
 436 simplified formulae of veblenite as the sum of the cation and anion components:

437 K<sub>2</sub>□<sub>2</sub>Na(Fe<sup>2+</sup><sub>5</sub>Fe<sup>3+</sup><sub>4</sub>Mn<sup>2+</sup><sub>7</sub>□)Nb<sub>3</sub>Ti(Si<sub>2</sub>O<sub>7</sub>)<sub>2</sub>(Si<sub>8</sub>O<sub>22</sub>)<sub>2</sub>O<sub>6</sub>(OH)<sub>10</sub>(H<sub>2</sub>O)<sub>3</sub> and (K,Ba,□)<sub>3</sub>(□,Na)<sub>2</sub>

438  $(\text{Fe}^{2+}, \text{Fe}^{3+}, \text{Mn}^{2+})_{17}(\text{Nb}, \text{Ti})_4(\text{Si}_2\text{O}_7)_2(\text{Si}_8\text{O}_{22})_2\text{O}_6(\text{OH})_{10}(\text{H}_2\text{O})_3$ , respectively,  $Z = 1$ . The validity of the  
 439 ideal formula is supported by the good agreement between the total charges for cations in the  
 440 ideal and empirical formulae:  $3^+ [\text{K}_2\text{□}_2\text{Na}] + 36^+ [\text{Fe}^{2+}_5\text{Fe}^{3+}_4\text{Mn}^{2+}_7\text{□}] + 19^+ [\text{Nb}_3\text{Ti}] = 58^+$  versus  $3^+$   
 441  $[\text{□}_{2.48}\text{K}_{1.25}\text{Na}_{0.72}\text{Ba}_{0.28}\text{Ca}_{0.17}\text{Cs}_{0.07}\text{Sr}_{0.03}] + 36.81^+ [(\text{Mn}^{2+}_{5.97}\text{Fe}^{2+}_{5.32}\text{Fe}^{3+}_{4.13}\text{Ca}_{0.70}\text{□}_{0.66}\text{Zn}_{0.15}\text{Mg}_{0.07})]$   
 442  $+ 18.73^+ [(\text{Nb}_{2.90}\text{Ti}_{0.93}\text{Fe}^{2+}_{0.17})] = 58.54^+$ .

443

#### 444 **The general structural formula of veblenite**

445 Above, we wrote the ideal formulae of veblenite based on the sum of the cation and anion  
 446 components:  $\text{K}_2\text{□}_2\text{Na}(\text{Fe}^{2+}_5\text{Fe}^{3+}_4\text{Mn}^{2+}_7\text{□})\text{Nb}_3\text{Ti}(\text{Si}_2\text{O}_7)_2(\text{Si}_8\text{O}_{22})_2\text{O}_6(\text{OH})_{10}(\text{H}_2\text{O})_3$ ,  $Z = 1$ . The  
 447 structural formula has the form  $\text{A}_1\text{A}_2\text{B}_2\text{M}_{17}\text{D}_4(\text{Si}_2\text{O}_7)_2(\text{Si}_8\text{O}_{22})_2\text{X}^{\text{O}}_{\text{D}4}\text{X}^{\text{P}}_{\text{D}2}\text{X}^{\text{O}}_{\text{A}10}\text{W}_8$  where A and B are  
 448 interstitial cations; M and D are cations of the O and H sheets;  $\text{X}^{\text{O}}$  are anions of the O sheet;  $\text{X}^{\text{P}}_{\text{D}}$   
 449 are common anions for the D cations and from two adjacent HOH layers; and W are  $\text{H}_2\text{O}$  groups  
 450 in the wide channels. The structural formula obtained from chemical analysis (Table 2) is  
 451 therefore  $(\text{K}_{0.53}\text{Ba}_{0.28}\text{Sr}_{0.03}\text{□}_{0.16})_{\Sigma 1}(\text{K}_{0.72}\text{Cs}_{0.07}\text{□}_{1.21})_{\Sigma 2}(\text{Na}_{0.72}\text{Ca}_{0.18}\text{□}_{1.10})_{\Sigma 2}(\text{Fe}^{2+}_{5.32}\text{Fe}^{3+}_{4.13}\text{Mn}^{2+}_{5.97}$   
 452  $\text{Ca}_{0.70}\text{Zn}_{0.15}\text{Mg}_{0.07}\text{□}_{0.66})_{\Sigma 17}(\text{Nb}_{2.90}\text{Ti}_{0.93}\text{Fe}^{3+}_{0.17})_{\Sigma 4}(\text{Si}_2\text{O}_7)_2(\text{Si}_{7.80}\text{Al}_{0.20}\text{O}_{22})_2\text{O}_6(\text{OH}_{9.78}\text{F}_{0.22})_{\Sigma 10}(\text{H}_2\text{O})_2$   
 453  $[(\text{H}_2\text{O})_{1.23}\text{□}_{2.77}]_{\Sigma 4}$ . The ideal formulae of veblenite,  $\text{K}_2\text{□}_2\text{Na}(\text{Fe}^{2+}_5\text{Fe}^{3+}_4\text{Mn}^{2+}_7\text{□})\text{Nb}_3\text{Ti}(\text{Si}_2\text{O}_7)_2$   
 454  $(\text{Si}_8\text{O}_{22})_2\text{O}_6(\text{OH})_{10}(\text{H}_2\text{O})_3$ , requires  $\text{Nb}_2\text{O}_5$  12.76,  $\text{TiO}_2$  2.56,  $\text{SiO}_2$  38.46,  $\text{Fe}_2\text{O}_3$  10.22,  $\text{MnO}$  15.89,  
 455  $\text{FeO}$  11.50,  $\text{K}_2\text{O}$  3.01,  $\text{Na}_2\text{O}$  0.99,  $\text{H}_2\text{O}$  4.61; total 100.00 wt.%. The simplified formula of  
 456 veblenite is  $(\text{K}, \text{Ba}, \text{□})_3(\text{□}, \text{Na})_2(\text{Fe}^{2+}, \text{Fe}^{3+}, \text{Mn}^{2+})_{17}(\text{Nb}, \text{Ti})_4(\text{Si}_2\text{O}_7)_2(\text{Si}_8\text{O}_{22})_2\text{O}_6(\text{OH})_{10}(\text{H}_2\text{O})_3$ .

457

#### 458 **Summary**

459 Veblenite is a new (Nb,Ti)-silicate mineral with a new structure that has no natural or synthetic  
 460 analogues. It is triclinic: space group  $P\bar{1}$ ,  $a$  5.3761(3),  $b$  27.5062(11),  $c$  18.6972(9) Å,  $\alpha$   
 461 140.301(3),  $\beta$  93.033(3),  $\gamma$  95.664(3)°,  $V = 1720.96(14)$  Å<sup>3</sup>. The structural unit of veblenite is an  
 462 HOH layer. Dominant cations in the O sheet are  $(\text{Fe}^{2+} + \text{Fe}^{3+}) > \text{Mn}^{2+}$ , with  $\text{Fe}^{2+} > \text{Fe}^{3+}$ . The H

463 sheet is composed of (Nb,Ti) octahedra, Si<sub>2</sub>O<sub>7</sub> groups and the veblenite Si<sub>8</sub>O<sub>22</sub> ribbon, a new  
464 type of Si-O ribbon. In the structure, the HOH layers connect via common anions of (Nb,Ti)  
465 octahedra. In the interstitial space between two HOH layers, K and Na atoms and H<sub>2</sub>O groups  
466 constitute the I block.

467 We write the ideal and simplified formulae of veblenite (Z = 1) as

468  $K_2\Box_2Na(Fe^{2+}_5Fe^{3+}_4Mn^{2+}_7\Box)Nb_3Ti(Si_2O_7)_2(Si_8O_{22})_2O_6(OH)_{10}(H_2O)_3$  and

469  $(K,Ba,\Box)_3(\Box,Na)_2(Fe^{2+},Fe^{3+},Mn^{2+})_{17}(Nb,Ti)_4(Si_2O_7)_2(Si_8O_{22})_2O_6(OH)_{10}(H_2O)_3$ , respectively.

470 Aspects of the crystal chemistry of veblenite will be considered in a later paper.

471

## 472 **Acknowledgements**

473 **We thank Jeffrey Post and Ian Grey for reviewing the manuscript.** FCH was supported by a  
474 Canada Research Chair in Crystallography and Mineralogy, by Discovery and Major Installation  
475 grants from the Natural Sciences and Engineering Research Council of Canada, and by  
476 Innovation Grants from the Canada Foundation for Innovation. FC also thanks Frank Hawthorne  
477 for supporting a visiting research period at Winnipeg.

478

479 **References**

- 480 Brown, I.D. (1981) The bond-valence method: an empirical approach to chemical structure and  
481 bonding. Pp. 1-30 in: *Structure and Bonding in Crystals II* (M. O'Keeffe and A. Navrotsky,  
482 editors). Academic Press, New York.
- 483 Cámara, F. and Sokolova, E. (2007) From structure topology to chemical composition. VI.  
484 Titanium silicates: the crystal structure and crystal chemistry of bornemanite, a group-III  
485 Ti-disilicate mineral. *Mineralogical Magazine*, **71**, 593-610.
- 486 Cámara, F. and Sokolova, E. (2009) From structure topology to chemical composition. X.  
487 Titanium silicates: the crystal structure and crystal chemistry of nechelyustovite, a group  
488 III Ti-disilicate mineral. *Mineralogical Magazine*, **73**, 887-897.
- 489 Cámara, F., Sokolova, E., Abdu, Y. and Hawthorne, F.C. (2010) The crystal structures of  
490 niobophyllite, kupletskite-(Cs) and Sn-rich astrophyllite; revisions to the crystal chemistry  
491 of the astrophyllite-group minerals. *The Canadian Mineralogist*, **48**, 1-16.
- 492 Cámara, F., Sokolova, E. and Hawthorne, F.C. (2012) Kazanskyite,  $\text{Ba}\square\text{TiNbNa}_3\text{Ti}(\text{Si}_2\text{O}_7)_2\text{O}_2$   
493  $(\text{OH})_2(\text{H}_2\text{O})_4$ , a Group-III Ti-disilicate mineral from the Khibiny alkaline massif, Kola  
494 Peninsula, Russia: description and crystal structure. *Mineralogical Magazine*, **76**, 473-  
495 492.
- 496 Ercit, T.S., Cooper, M.A. and Hawthorne, F.C. (1998) The crystal structure of vuonnemite,  
497  $\text{Na}_{11}\text{Ti}^{4+}\text{Nb}_2(\text{Si}_2\text{O}_7)_2(\text{PO}_4)_2\text{O}_3(\text{F},\text{OH})$ , a phosphate-bearing sorosilicate of the  
498 lomonosovite group. *The Canadian Mineralogist*, **36**, 1311-1320.
- 499 Ferraris, G. (2008) Modular structures – the paradigmatic case of the heterophyllosilicates.  
500 *Zeitschrift für Kristallographie*, **223**, 76-84.
- 501 Ferraris, G., Ivaldi, G., Khomyakov, A.P., Soboleva, S.V., Belluso, E. and Pavese, A. (1996)  
502 Nafertisite, a layer titanosilicate member of a polysomatic series including mica.  
503 *European Journal of Mineralogy*, **8**, 241-249.

504 Hawthorne, F.C. (2012) Bond topology and structure-generating functions: graph-theoretic  
505 prediction of chemical composition and structure in polysomatic T-O-T (biopyribole) and  
506 H-O-H structures. *Mineralogical Magazine*, **76**, 1053-1080.

507 Hong, W. and Fu, P. (1982) Jinshajiangite, a new Ba-Mn-Fe-Ti-bearing silicate mineral.  
508 *Geochemistry (China)*, **1**, 458-464.

509 Khomyakov, A.P., Ferraris, G., Ivaldi, G., Nechelyustov, G.N. and Soboleva, S.V. (1995)  
510 Nafertisite,  $\text{Na}_3(\text{Fe}^{2+}, \text{Fe}^{3+})_6[\text{Ti}_2\text{Si}_{12}\text{O}_{34}](\text{O}, \text{OH})_7 \cdot 2\text{H}_2\text{O}$ , a new mineral with a new type of  
511 banded silicate radical. *Zapiski Vserossiyskogo Mineralogicheskogo Obshchestva*, **124**,  
512 101-107 (in Russian).

513 Nickel, E.H., Rowland, J.F. and Charette, D.J. (1964) Niobophyllite-the niobium analogue of  
514 astrophyllite; a new mineral from Seal Lake, Labrador. *The Canadian Mineralogist*, **8**, 40-  
515 52.

516 Pouchou, J.L. and Pichoir, F. (1985) 'PAP'  $\phi(\rho Z)$  procedure for improved quantitative  
517 microanalysis. Pp. 104-106 in: *Microbeam Analysis* (J.T. Armstrong, editor). San  
518 Francisco Press, San Francisco, California, USA.

519 Rowe, R. (2009) New statistical calibration approach for Bruker AXS D8 Discover  
520 microdiffractometer with Hi-Star detector using GADDS software, *ICDD Powder*  
521 *diffraction Journal*, **24**, 263-271.

522 Shannon, R.D. (1976) Revised effective ionic radii and systematic studies of interatomic  
523 distances in halides and chalcogenides. *Acta Crystallographica*, **A32**, 751-767.

524 Sheldrick, G.M. (2008) A short history of SHELX. *Acta Crystallographica*, **A64**, 112-122.

525 Sokolova, E. (2006) From structure topology to chemical composition. I. Structural hierarchy  
526 and stereochemistry in titanium disilicate minerals. *The Canadian Mineralogist*, **44**, 1273-  
527 1330.

528 Sokolova, E. (2012) Further developments in the structure topology of the astrophyllite-group  
529 minerals. *Mineralogical Magazine*, **76**, 863-882.

- 530 Sokolova, E. and Hawthorne, F.C. (2004) The crystal chemistry of epistolite. *The Canadian*  
531 *Mineralogist*, **42**, 797-806.
- 532 Sokolova, E., Cámara, F., Hawthorne, F.C. and Abdu, Y. (2009) From structure topology to  
533 chemical composition. VII. Titanium silicates: the crystal structure and crystal chemistry  
534 of jinshajiangite. *European Journal of Mineralogy*, **21**, 871-883.
- 535 Wilson, A.J.C. (editor) (1992) International Tables for Crystallography. Volume C: Mathematical,  
536 physical and chemical. Kluwer Academic Publishers, Dordrecht, The Netherlands.
- 537

538 **Figure captions**

539

540 **FIG. 1.** Images of veblenite crystals (marked with arrows) in albite (ab) matrix in probe  
541 mounting.

542

543 **FIG. 2.** IR spectrum of veblenite.

544

545 **FIG. 3.** General view of the crystal structure of veblenite. Si tetrahedra are orange, Fe<sup>2+</sup>-, Fe<sup>3+</sup>-  
546 and Mn-dominant M octahedra are green, yellow and pink, (Nb,Ti) D octahedra are pale yellow;  
547 K- and Na- dominant A(1), A(2) and B sites are shown as green and blue spheres, respectively;  
548 OH and H<sub>2</sub>O groups are shown as small and large red spheres. The unit cell is shown with thin  
549 black lines.

550

551 **FIG. 4.** The HOH layer in veblenite (a) The O sheet; (b) The H sheet in veblenite shows two  
552 types of Si-O radicals: Si<sub>2</sub>O<sub>7</sub> groups and a new veblenite Si<sub>8</sub>O<sub>22</sub> ribbon; the repeat of the  
553 veblenite ribbon is indicated with a red box; (c) linkage of H and O sheets. Legend as in Fig. 3,  
554 Si tetrahedra are orange, (Nb,Ti) D octahedra are pale yellow. The unit cell is shown with thin  
555 black lines; in (c), M octahedra are numbered.

556

557 **FIG. 5.** General view of the narrow and wide [100]-channels in the structure of veblenite,  
558 showing the position of A and B sites and OH and H<sub>2</sub>O groups: (a) projection along [100]. (b)  
559 projection along [001] (legend as in Fig. 3).

560

561 **FIG. 6.** Fragment of the crystal structure showing details of the linkage of two HOH layers via  
562 the bridge D-X<sup>P</sup><sub>D</sub>-D. Nb and Na atoms at the D and B sites are shown as yellow and blue  
563 spheres, O atoms at the X<sup>P</sup><sub>D</sub> and X<sup>O</sup><sub>D</sub> sites are shown as red spheres, bonds between Nb and



564 Na atoms and O atoms are shown as solid black lines; Fe<sup>2+</sup> - and Mn-dominant octahedra in the

565 O sheet are green and magenta and represent O sheets of different HOH layers.

566

TABLE 1. Comparison of veblenite, jinshajiangite, niobophyllite and nafertisite.

Mineral	Veblenite	Jinshajiangite	Niobophyllite	Nafertisite
Reference*	(1)	(4, 8)	(2, 6, 7)	(3, 5)
Formula	$K_2\Box_2Na(Fe^{2+}_5Fe^{3+}_4Mn_7)Nb_3Ti(Si_2O_7)_2(Si_8O_{22})_2O_6(OH)_{10}(H_2O)_3$	$Ba_2Na_2Fe^{2+}_8Ti_4(Si_2O_7)_4O_4(OH,F)_6$	$K_2NaFe^{2+}_7(Nb,Ti)(Si_4O_{12})_2O_2(OH)_4(O,OH)$	$(Na,K)_3(Fe^{2,3+}\Box)_{10}Ti_2(Si_6O_{17})_2O_3(OH,O)_6$
System	Triclinic	Monoclinic	Triclinic	Monoclinic
Space group	$P\bar{1}$	$C2/m$	$P\bar{1}$	$A2/m$
$a(\text{\AA})$	5.3761	10.6785	5.4022	5.353
$b$	27.506	13.786	11.8844	16.18
$c$	18.6972	20.700	11.6717	21.95
$\alpha(^{\circ})$	140.301	90	112.990	90
$\beta$	93.033	94.937	94.588	94.6
$\gamma$	95.664	90	103.166	90
$V(\text{\AA}^3)$	1720.96	3035.93	659.7	1894.41
$Z$	1	4	1	2
$D_{\text{calc}}(\text{gcm}^{-3})$	3.041	3.767	3.406	2.83
$D_{\text{meas}}(\text{gcm}^{-3})$	n.d.	3.61	3.42	2.7
Strongest lines in the powder pattern, $d_{\text{obs}}(\text{\AA})(l)$	16.894 (100) 18.20 (23) 4.27 (9) 11.66 (8) 2.72 (3) 4.40 (3) 4.06 (3)	3.44 (100) 3.15 (80) 2.630 (80) 2.570 (80) 10.2 (70) 1.715 (50 broad) 2.202 (40)	3.506 (100) 10.52 (90) 2.778 (80) 2.574 (70) 3.019 (60) 3.258 (50) 2.475 (40)	10.94 (100) 13.00 (30) 2.728 (25) 2.641 (20) 2.547 (15) 2.480 (15) 3.638 (10)
optical class (sign)	biaxial (-)	biaxial (+)	biaxial (-)	biaxial (-)
$\alpha(589.3\text{ nm})$	1.635(2)	1.792	1.724	1.627
$\beta$	1.647(2)	1.801	1.760	1.667
$\gamma$	1.652(2)	1.852	1.772	1.693
$2V_{\text{meas}}(^{\circ})$	65.3(1.2)	72	60	75(2)
$2V_{\text{calc}}(^{\circ})$	65.3	–	–	76

\*Jinshajiangite: formula, unit-cell parameters, space group and calculated density (8); powder pattern,  $D_{\text{meas}}$  and optics (4); Niobophyllite: formula (7); unit-cell parameters, space group and calculated density (2);  $D_{\text{meas}}$ , powder pattern and optics (6); Nafertisite: formula, unit-cell parameters, space group and calculated density (3);  $D_{\text{meas}}$ , powder pattern and optics (5). n.d. = not determined.

References : (1) this work; (2) Cámara *et al.* (2010); (3) Ferraris *et al.* (1996); (4) Hong and Fu (1982); (5) Khomyakov *et al.* (1995); (6) Nickel *et al.* (1964); (7) Sokolova (2012); (8) Sokolova *et al.* (2009).

TABLE 2. Chemical composition and unit formula\* for veblenite

Oxide	wt. %	Formula	a.p.f.u. unit
Nb <sub>2</sub> O <sub>5</sub>	11.69	Si	19.61
TiO <sub>2</sub>	2.26	Al	<u>0.39</u>
SiO <sub>2</sub>	35.71	Σ	20.00
Al <sub>2</sub> O <sub>3</sub>	0.60		
Fe <sub>2</sub> O <sub>3</sub> **	10.40	Fe <sup>2+</sup>	5.32
FeO**	11.58	Fe <sup>3+</sup>	4.13
MnO	12.84	Mn <sup>2+</sup>	5.97
ZnO	0.36	Ca	0.70
MgO	0.08	Zn	0.15
BaO	1.31	Mg	<u>0.07</u>
SrO	0.09	Σ17M	16.34
CaO	1.49		
Cs <sub>2</sub> O	0.30	Nb	2.90
K <sub>2</sub> O	1.78	Ti	0.93
Na <sub>2</sub> O	0.68	Fe <sup>3+</sup>	<u>0.17</u>
H <sub>2</sub> O**	4.39	Σ4D	4.00
F	0.22		
-O=F <sub>2</sub>	<u>0.09</u>	Na	0.72
Total	95.69	Ca	<u>0.17</u>
		Σ B	0.89
		K	1.25
		Ba	0.28
		Cs	0.07
		Sr	<u>0.03</u>
		Σ3A	1.63
		F	0.38
		OH	<u>9.62</u>
		Σ	10.00
		H <sub>2</sub> O	3.23

\* calculated on cation basis: Si + Al = 20 a.p.f.u.;

\*\* calculated from structure solution and refinement: FeO(total) = 20.94 wt.%; OH + F = 10 p.f.u., H<sub>2</sub>O = 3.23 p.f.u.

TABLE 3. X-ray powder diffraction data for veblenite.\*

$l_{\text{obs.}}$	$d_{\text{obs}}$ (Å)	$d_{\text{calc}}$ (Å)	$l_{\text{calc}}$	$h$	$k$	$l$
22.7	18.204	18.382	75	0	$\bar{1}$	1
100	16.894	17.094	66	0	1	0
7.8	11.661	11.671	100	0	0	1
2.8	4.404	4.444	5	$\bar{1}$	$\bar{3}$	2
		4.404	3	1	$\bar{4}$	2
8.7	4.271	4.304	1	1	$\bar{4}$	1
		4.274	1.5	0	4	0
		4.097	1	1	2	0
2.7	4.056	4.031	1	0	3	1
		4.022	1	1	$\bar{1}$	2
		4.021	2	1	$\bar{5}$	2
		3.996	1	$\bar{1}$	$\bar{4}$	3
2.4	3.891	3.890	4	0	0	3
1.6	3.747	3.750	3	$\bar{1}$	4	0
1.6	3.340	3.340	7	0	$\bar{1}$	4
2.3	3.284	3.281	7	0	1	3
1.4	3.007	3.014	2	$\bar{1}$	$\bar{7}$	4
		3.009	2	1	$\bar{8}$	4
		3.009	2	1	4	0
2.9	2.721	2.721	6	1	$\bar{9}$	5
		2.720	6	$\bar{1}$	$\bar{8}$	4
2.2	2.627	2.628	2	$\bar{1}$	$\bar{7}$	2
		2.618	2	1	$\bar{8}$	6
2.1	2.557	2.562	4	1	$\bar{9}$	6
		2.557	4	$\bar{1}$	$\bar{8}$	3
1.3	2.324	2.329	1	1	$\bar{9}$	7
		2.322	1	$\bar{1}$	$\bar{8}$	2
1.9	2.163	2.152	1	1	$\bar{10}$	2
1.9	2.072	2.074	0.5	$\bar{1}$	$\bar{8}$	1
		2.072	0.5	$\bar{1}$	$\bar{9}$	2
1.5	2.046	2.049	1	1	7	0
		2.041	1	1	$\bar{8}$	8
1.8	1.8666	1.8659	0.5	1	$\bar{10}$	2
		1.8638	0.5	$\bar{1}$	$\bar{9}$	1
1.2	1.7533	1.7534	1	1	6	2

\* Indexed on  $a = 5.41(3)$ ,  $b = 27.36(5)$ ,  $c = 18.62(3)$  Å,  $\alpha = 140.17(8)$ ,  $\beta = 93.3(2)$ ,  $\gamma = 95.6(1)^\circ$ ,  $V = 1719(6)$  Å<sup>3</sup>;  $d_{\text{calc}}$ ,  $l_{\text{calc}}$  and  $hkl$  values are from the powder pattern calculated from single-crystal data.

TABLE 4. Miscellaneous refinement data for veblenite.

---

<i>a</i> (Å)	5.3761(3)
<i>b</i>	27.506(1)
<i>c</i>	18.697(1)
$\alpha$ (°)	140.301(2)
$\beta$	93.032(1)
$\gamma$	95.664(3)
<i>V</i> (Å <sup>3</sup> )	1720.96(14)
Space group	$P\bar{1}$
<i>Z</i>	1
Absorption coefficient (mm <sup>-1</sup> )	4.47
<i>F</i> (000)	1527.0
<i>D</i> <sub>calc.</sub> (g/cm <sup>3</sup> )	3.041
Crystal size (mm)	0.20 x 0.04 x 0.02
Radiation/filter	Mo-K $\alpha$ /graphite
2 $\theta$ <sub>max</sub> for structure refinement (°)	46.00
<i>R</i> (int) (%)	6.65
Reflections collected	16.431
Independent reflections	4777
<i>F</i> <sub>o</sub> > 4 $\sigma$ <i>F</i>	3329
Refinement method	Full-matrix least squares on <i>F</i> <sup>2</sup> , fixed weights proportional to 1/ $\sigma$ <i>F</i> <sub>o</sub> <sup>2</sup>
No. of refined parameters	369
Final <i>R</i> (obs) (%)	
[ <i>F</i> <sub>o</sub> > 4 $\sigma$ <i>F</i> ]	9.09
<i>R</i> <sub>1</sub>	12.02
<i>wR</i> <sub>2</sub>	23.20
Highest peak, deepest hole	1.90
(e Å <sup>-3</sup> )	1.34
Goodness of fit on <i>F</i> <sup>2</sup>	1.100

---

TABLE 5. Final atom coordinates and displacement parameters ( $\text{\AA}^2$ ) for veblenite.

Atom	Site occ. (%)	x	y	z	$U_{\text{iso}}^*$
Si(1)	100	0.9550(9)	0.3400(3)	0.2837(4)	0.0110(12)
Si(2)	100	0.4407(9)	0.2992(3)	0.3066(4)	0.0096(11)
Si(3)	100	0.3956(10)	0.2023(3)	0.3330(4)	0.0140(12)
Si(4)	100	0.8699(10)	0.1504(3)	0.3351(4)	0.0137(12)
Si(5)	100	0.1114(8)	0.6614(3)	0.1994(4)	0.0019(10)
Si(6)	100	0.2164(8)	0.8294(3)	0.2430(4)	0.0044(10)
Si(7)	100	0.2782(10)	0.9679(3)	0.3005(4)	0.0126(12)
Si(8)	100	0.1849(9)	0.9672(3)	0.6785(4)	0.0138(12)
Si(9)	100	0.9889(8)	0.5780(3)	0.7670(4)	0.0033(10)
Si(10)	100	0.9462(8)	0.4522(3)	0.8048(4)	0.0009(10)
D(1A)	50	0.6507(9)	0.7277(3)	0.1852(4)	0.0021(16)
D(1B)	50	0.6366(8)	0.7140(3)	0.1559(5)	0.0021(7)
D(2A)	50	0.4996(9)	0.5522(7)	0.8505(12)	0.0021(7)
D(2B)	50	0.4862(13)	0.5355(10)	0.8217(17)	0.0021(7)
M(1)	100	$\frac{1}{2}$	0	$\frac{1}{2}$	0.0058(9)
M(2)	100	0.6415(4)	0.27139(14)	0.5679(2)	0.0077(6)
M(3)	100	0.7330(4)	0.47901(15)	0.5129(2)	0.0082(7)
M(4)	100	0.8706(5)	0.78595(15)	0.4275(2)	0.0111(7)
M(5)	100	0.1885(5)	0.33821(15)	0.5775(2)	0.0136(7)
M(6)	100	0.9518(5)	0.92035(16)	0.4611(2)	0.0164(7)
M(7)	85	0.7035(6)	0.3899(2)	0.5641(3)	0.0114(8)
M(8)	97	0.2361(6)	0.4400(2)	0.5521(3)	0.0287(9)
M(9)	85	0.4225(7)	0.8513(2)	0.4410(3)	0.0179(9)
A(1)	83	$\frac{1}{2}$	$\frac{1}{2}$	0	0.0334(17)
A(2A)	10	0.645(12)	0.751(4)	0.007(4)	0.0334(17)
A(2B)	10	0.502(11)	0.751(3)	-0.003(4)	0.0334(17)
A(2C)	10	0.786(13)	0.759(3)	0.008(4)	0.0334(17)
A(2D)	10	0.640(8)	0.765(3)	0.999(4)	0.0334(17)
B	44	0.075(3)	0.6442(11)	0.0033(17)	0.0334(17)
O(1)	100	0.610(3)	0.1508(9)	0.2902(12)	0.034(4)
O(2)	100	0.106(3)	0.1559(9)	0.2914(12)	0.033(4)
O(3)	100	0.409(2)	0.2264(8)	0.2770(11)	0.023(3)
O(4)	100	0.169(3)	0.2921(8)	0.2517(12)	0.028(3)
O(5)	100	0.674(3)	0.2927(8)	0.2482(12)	0.028(3)
O(6)	100	0.336(2)	0.6686(8)	0.1557(11)	0.020(3)
O(7)	100	0.840(2)	0.6550(7)	0.1505(10)	0.016(3)
O(8)	100	0.947(3)	0.7701(8)	0.1776(11)	0.027(3)
O(9)	100	0.446(3)	0.7849(9)	0.1904(13)	0.037(4)
O(10)	100	0.224(2)	0.8787(7)	0.2257(10)	0.018(3)
O(11)	100	0.929(2)	0.2239(7)	0.4753(10)	0.013(3)
O(12)	100	0.463(2)	0.2767(7)	0.4721(10)	0.015(3)
O(13)	100	0.516(2)	0.3798(7)	0.4433(9)	0.009(3)
O(14)	100	0.019(2)	0.4234(6)	0.4200(9)	0.007(3)
O(15)	100	0.168(2)	0.7335(7)	0.3381(10)	0.012(3)
O(16)	100	0.262(2)	0.8908(7)	0.3812(10)	0.014(3)
O(17)	100	0.665(2)	0.9708(7)	0.5625(10)	0.009(3)

TABLE 5. continued.

Atom	Site occ. (%)	x	y	z	$U_{iso}^*$
O(18)	100	0.117(2)	0.8979(7)	0.5387(9)	0.009(3)
O(19)	100	0.924(2)	0.4952(7)	0.6295(11)	0.019(3)
O(20)	100	0.886(2)	0.3794(7)	0.6669(10)	0.014(3)
O(21)	100	0.909(2)	0.4196(8)	0.8494(11)	0.022(3)
O(22)	100	0.755(2)	0.5068(7)	0.8520(11)	0.019(3)
O(23)	100	0.232(2)	0.4986(8)	0.8535(11)	0.021(3)
O(24)	100	0.751(2)	0.5900(8)	0.8223(11)	0.024(3)
O(25)	100	0.238(3)	0.5840(8)	0.8247(12)	0.030(4)
O(26)	100	0.045(2)	0.6490(7)	0.7894(10)	0.011(3)
O(27)	100	0.165(3)	0.9313(8)	0.7159(12)	0.031(4)
O(28)	100	0.474(3)	0.0178(10)	0.7312(14)	0.044(4)
O(29)	100	0.971(3)	0.0226(9)	0.7353(13)	0.035(4)
X <sub>D</sub> <sup>O</sup> (1)	100	0.726(2)	0.8043(8)	0.3449(11)	0.021(3)
X <sub>D</sub> <sup>O</sup> (2)	100	0.416(2)	0.4431(8)	0.6639(11)	0.023(3)
X <sub>A</sub> <sup>O</sup> (1)	100	0.003(2)	0.3369(7)	0.4758(10)	0.017(3)
X <sub>A</sub> <sup>O</sup> (2)	100	0.207(2)	0.0383(7)	0.5868(10)	0.016(3)
X <sub>A</sub> <sup>O</sup> (3)	100	0.591(2)	0.8311(7)	0.5224(10)	0.010(3)
X <sub>A</sub> <sup>U</sup> (4)	100	0.456(2)	0.5325(7)	0.5968(10)	0.013(3)
X <sub>A</sub> <sup>O</sup> (5)	100	0.357(2)	0.3192(7)	0.6549(11)	0.019(3)
X <sub>D</sub> <sup>P</sup>	100	0.5700(19)	0.6418(6)	0.0038(9)	0.004(2)
W(1)	57	0.814(6)	0.1264(18)	0.106(3)	0.05**
W(2)	43	0.745(8)	0.013(2)	0.885(3)	0.05**
W(3)	23	0.734(15)	0.160(4)	0.990(6)	0.05**
W(4)	17	0.623(18)	0.864(6)	0.997(8)	0.05**
W(5)	21	0.941(16)	0.160(5)	0.989(7)	0.05**
Subsidiary peaks					
M(1A) <sup>‡</sup>	5	0.521(9)	-0.008(3)	0.457(5)	0.01**
M(6A)	2	0.91(2)	0.875(8)	0.358(12)	0.01**
M(9A)	6	0.474(8)	0.917(3)	0.586(4)	0.01**

\*  $U_{eq}$  for Si(1-8), M(2-9), A(1), A(2A-2D), B; \*\* fixed; † scattering curves of Fe<sup>2+</sup>, Fe<sup>2+</sup> and Mn were used in the refinement of site occupancies of M(1A), M(6A) and M(9A), respectively.

TABLE 6. Selected interatomic distances (Å) and angles (°) in veblenite.

Si(1)-O(4)d	1.61(1)	Si(2)-O(3)	1.60(1)	Si(3)-O(3)	1.61(1)	Si(4)-O(1)	1.59(2)
Si(1)-O(26)c	1.61(1)	Si(2)-O(13)	1.61(1)	Si(3)-O(2)	1.62(1)	Si(4)-O(2)d	1.60(2)
Si(1)-O(5)	1.61(1)	Si(2)-O(5)	1.64(1)	Si(3)-O(12)	1.63(1)	Si(4)-O(27)c	1.61(2)
Si(1)-O(14)d	<u>1.62(1)</u>	Si(2)-O(4)	<u>1.65(1)</u>	Si(3)-O(1)	1.63(2)	Si(4)-O(11)	<u>1.64(1)</u>
<Si(1)-O>	1.61	<Si(2)-O>	1.63	<Si(3)-O>	1.62	<Si(4)-O>	1.61
Si(5)-O(6)	1.57(1)	Si(6)-O(8)a	1.59(1)	Si(7)-O(29)c	1.60(2)	Si(8)-O(27)	1.59(2)
Si(5)-O(7)a	1.60(1)	Si(6)-O(9)	1.60(2)	Si(7)-O(10)	1.61(1)	Si(8)-O(28)k	1.62(2)
Si(5)-O(21)c	1.62(1)	Si(6)-O(10)	1.62(1)	Si(7)-O(28)c	1.62(2)	Si(8)-O(18)	1.64(1)
Si(5)-O(15)	<u>1.62(1)</u>	Si(6)-O(16)	<u>1.65(1)</u>	Si(7)-O(17)f	<u>1.63(1)</u>	Si(8)-O(29)o	<u>1.66(2)</u>
<Si(5)-O>	1.60	<Si(6)-O>	1.62	<Si(7)-O>	1.62	<Si(8)-O>	1.63
Si(9)-O(24)	1.59(1)	Si(10)-O(22)	1.57(1)	Si(3)-O(1)-Si(4)	142.6(1.0)		
Si(9)-O(25)d	1.59(1)	Si(10)-O(23)d	1.58(1)	Si(3)-O(2)-Si(4)a	143.4(1.0)		
Si(9)-O(19)	1.63(1)	Si(10)-O(20)	1.61(1)	Si(2)-O(3)-Si(3)	143.3(9)		
Si(9)-O(26)d	<u>1.64(1)</u>	Si(10)-O(21)	<u>1.63(1)</u>	Si(1)a-O(4)-Si(2)	142.4(1.0)		
<Si(9)-O>	1.61	<Si(10)-O>	1.60	Si(1)-O(5)-Si(2)	140.3(1.0)		
				Si(6)-O(10)-Si(7)	139.9(8)		
				Si(5)-O(21)-Si(10)	139.1(1.9)		
				Si(1)-O(26)-Si(9)	138.8(8)		
				Si(4)c-O(27)-Si(8)	142.0(1.0)		
				Si(7)c-O(28)-Si(8)f	143.4(1.1)		
				Si(7)c-O(29)-Si(8)g	141.1(1.0)		
D(1A)-X <sup>O</sup> <sub>D</sub> (1)	1.88(1)	D(1B)-X <sup>P</sup> <sub>D</sub>	1.79(1)	D(2A)-X <sup>P</sup> <sub>Db</sub>	1.81(2)	D(2B)-X <sup>O</sup> <sub>D</sub> (2)	1.86(2)
D(1A)-O(6)	1.95(1)	D(1B)-O(6)	1.94(1)	D(2A)-O(25)	1.95(1)	D(2B)-O(25)	1.95(2)
D(1A)-O(9)	1.95(2)	D(1B)-O(8)	1.95(1)	D(2A)-O(24)	1.96(1)	D(2B)-O(24)	1.96(1)
D(1A)-O(8)	1.96(1)	D(1B)-O(9)	1.95(2)	D(2A)-O(22)	1.96(1)	D(2B)-O(22)	1.96(1)
D(1A)-O(7)	1.98(1)	D(1B)-O(7)	1.99(1)	D(2A)-O(23)	1.99(1)	D(2B)-O(23)	2.00(1)
D(1A)-X <sup>P</sup> <sub>D</sub>	<u>2.14(1)</u>	D(1B)-X <sup>O</sup> <sub>D</sub> (1)	<u>2.23(1)</u>	D(2A)-X <sup>O</sup> <sub>D</sub> (2)	<u>2.20(2)</u>	D(2B)-X <sup>P</sup> <sub>Db</sub>	<u>2.15(2)</u>
<D(1A)-O>	1.98	<D(1B)-O>	1.98	<D(2A)-O>	1.98	<D(2B)-O>	1.98
M(1)-X <sup>O</sup> <sub>A</sub> (2)	2.05(1)	x2 M(2)-X <sup>O</sup> <sub>A</sub> (5)	2.02(1)	M(3)-X <sup>O</sup> <sub>A</sub> (4)	1.99(1)	M(4)-X <sup>O</sup> <sub>A</sub> (3)	2.05(1)
M(1)-O(16)e	2.07(1)	x2 M(2)-X <sup>O</sup> <sub>A</sub> (3)c	2.03(1)	M(3)-X <sup>O</sup> <sub>A</sub> (4)c	2.01(1)	M(4)-X <sup>O</sup> <sub>D</sub> (1)	2.10(1)
M(1)-O(17)c	<u>2.07(1)</u>	x2 M(2)-O(11)	2.07(1)	M(3)-O(19)	2.05(1)	M(4)-O(15)d	2.11(1)
<M(1)-O>	2.06	M(2)-O(15)c	2.09(1)	M(3)-O(13)	2.06(1)	M(4)-X <sup>O</sup> <sub>A</sub> (5)c	2.12(1)
		M(2)-O(12)	2.10(1)	M(3)-O(14)d	2.09(1)	M(4)-O(18)d	2.15(1)
		M(2)-O(20)	<u>2.12(1)</u>	M(3)-O(14)c	<u>2.12(1)</u>	M(4)-O(11)j	<u>2.27(1)</u>
		<M(2)-O>	2.07	<M(3)-O>	2.05	<M(4)-O>	2.13
M(5)-X <sup>O</sup> <sub>A</sub> (1)	2.07(1)	M(6)-O(16)d	2.08(1)	M(7)-X <sup>O</sup> <sub>A</sub> (1)d	2.12(1)	M(8)-X <sup>O</sup> <sub>A</sub> (1)	2.13(1)
M(5)-X <sup>O</sup> <sub>A</sub> (5)	2.08(1)	M(6)-X <sup>O</sup> <sub>A</sub> (2)c	2.12(1)	M(7)-X <sup>O</sup> <sub>D</sub> (2)	2.14(1)	M(8)-X <sup>O</sup> <sub>A</sub> (4)	2.14(1)
M(5)-X <sup>O</sup> <sub>D</sub> (2)	2.09(1)	M(6)-O(17)	2.14(1)	M(7)-O(13)	2.22(1)	M(8)-O(19)a	2.14(1)
M(5)-O(20)a	2.11(1)	M(6)-O(18)d	2.15(1)	M(7)-O(19)	2.24(1)	M(8)-O(13)	2.19(1)
M(5)-O(12)	2.14(1)	M(6)-X <sup>O</sup> <sub>D</sub> (1)	2.16(1)	M(7)-O(12)	2.25(1)	M(8)-X <sup>O</sup> <sub>D</sub> (2)	2.19(1)
M(5)-O(11)a	<u>2.26(1)</u>	M(6)-X <sup>O</sup> <sub>A</sub> (2)p	<u>2.23(1)</u>	M(7)-O(20)	<u>2.33(1)</u>	M(8)-O(14)	<u>2.35(1)</u>
<M(5)-O>	2.13	<M(6)-O>	2.15	<M(7)-O>	2.22	<M(8)-O>	2.19



TABLE 6. continued

M(9)-X <sup>O</sup> <sub>A</sub> (3)	2.17(1)	A(1)-O(7)	2.98(1)	x2	A(2A)-X <sup>P</sup> <sub>D</sub>	2.94(9)	A(2B)-W(3)c	2.71(9)
M(9)-X <sup>O</sup> <sub>D</sub> (1)	2.17(1)	A(1)-O(23)i	3.00(1)	x2	A(2A)-O(24)i	3.00(7)	A(2B)-O(25)i	3.00(5)
M(9)-O(18)	2.19(1)	A(1)-O(21)i	3.11(1)	x2	A(2A)-O(9)j	3.07(8)	A(2B)-O(9)	3.01(5)
M(9)-O(17)	2.24(1)	A(1)-O(22)i	3.27(1)	x2	A(2A)-W(5)	3.09(12)	A(2B)-W(4)i	3.12(11)
M(9)-O(16)	2.26(1)	A(1)-O(21)h	3.32(1)	x2	A(2A)-O(8)	3.13(8)	A(2B)-O(26)i	3.14(5)
M(9)-O(15)	<u>2.31(1)</u>	A(1)-O(6)	<u>3.32(1)</u>	x2	A(2A)-O(25)i	3.26(7)	A(2B)-X <sup>P</sup> <sub>D</sub>	3.17(5)
<M(9)-O>	2.22	<A(1)-O>	3.17		A(2A)-W(4)i	3.29(14)	A(2B)-O(10)	3.39(5)
					A(2A)-W(3)c	3.30(12)	A(2B)-O(24)i	3.39(5)
					A(2A)-O(10)d	<u>3.63(6)</u>	A(2B)-W(5)c	3.44(10)
					<A(2A)-O>	3.19	A(2B)-W(5)j	<u>3.50(10)</u>
							<A(2B)-O>	3.19
							B-O(8)a	2.54(2)
A(2C)-W(5)j	2.51(10)	A(2D)-W(5)n	2.76(11)	Short distances			B-O(25)i	2.60(2)
A(2C)-O(24)i	2.93(6)	A(2D)-W(4)	2.77(13)				B-O(6)	2.64(2)
A(2C)-O(8)	3.01(5)	A(2D)-W(3)m	2.91(10)	D(1A)-D(1B)	0.345(6)		B-O(22)h	2.65(2)
A(2C)-O(10)d	3.13(6)	A(2D)-O(24)	3.29(6)	D(2A)-D(2B)	0.338(8)		B-X <sup>P</sup> <sub>D</sub>	2.67(2)
A(2C)-O(26)l	3.19(6)	A(2D)-O(9)b	3.43(7)	A(2A)-A(2B)	0.78(6)		B-X <sup>P</sup> <sub>Da</sub>	2.71(2)
A(2C)-W(3)j	3.22(10)	A(2D)-X <sup>P</sup> <sub>D</sub> b	3.46(8)	A(2A)-A(2C)	0.76(6)		B-O(24)h	2.80(2)
A(2C)-X <sup>P</sup> <sub>D</sub>	3.25(6)	A(2D)-O(25)	3.51(6)	A(2B)-A(2C)	1.50(7)		B-O(9)	2.85(2)
A(2C)-W(4)i	3.27(11)	A(2D)-O(8)b	3.55(7)	A(2B)-A(2D)i	0.79(6)		B-O(23)i	2.87(2)
A(2C)-O(9)	<u>3.55(6)</u>	A(2D)-O(26)	<u>3.63(4)</u>	A(2C)-A(2D)i	0.86(7)		B-O(7)	<u>2.91(2)</u>
<A(2C)-O>	3.12	<A(2D)-O>	3.26				<B-O>	<u>2.72</u>

Symmetry operators: a: x-1, y, z; b: x, y, z+1; c: -x+1, -y+1, -z+1; d: x+1, y, z; e: x, y-1, z; f: -x+1, -y+2, -z+1; g: x+1, y-1, z; h: x-1, y, z-1; i: x, y, z-1; j: -x+2, -y+1, -z+1; k: x, y+1, z; l: x+1, y, z-1; m: -x+1, -y+1, -z+2; n: -x+2, -y+1, -z+2; o: x-1, y+1, z; p: x+1, y+1, z,

TABLE 7. Refined site-scattering (e.p.f.u.) and assigned site-populations (a.p.f.u.) for veblenite\*.

Site**	Refined site-scattering	Site population	Calculated site-scattering	$\langle X-\varphi \rangle_{\text{calc.}}$ (Å)	$\langle X-\varphi \rangle_{\text{obs.}}$ (Å)
<i>D</i> (1A)	35.02(6)	0.55 Nb + 0.28 Ti + 0.17 Fe <sup>3+</sup> + 1.00 □	33.10	2.01	1.98
<i>D</i> (1B)	41.1(6)	0.90 Nb + 0.10 Ti + 1.00 □	37.20	2.02	1.98
<i>D</i> (2A)	45.8(3.0)	1.00 Nb + 1.00 □	41.00	2.02	1.98
<i>D</i> (2B)	31.5(3.0)	0.55 Ti + 0.45 Nb + 1.00 □	30.60	2.00	1.98
Total <i>D</i>	153.42	2.90 Nb + 0.93 Ti + 0.17 Fe <sup>3+</sup>	141.19		
<i>M</i> (1)	26.0	0.67 Fe <sup>3+</sup> + 0.33 Fe <sup>2+</sup>	26.00	2.06	2.06
<i>M</i> (2)	52.0	1.34 Fe <sup>3+</sup> + 0.66 Fe <sup>2+</sup>	52.00	2.06	2.07
<i>M</i> (3)	52.0	1.34 Fe <sup>3+</sup> + 0.66 Fe <sup>2+</sup>	52.00	2.06	2.05
<i>M</i> (4)	52.0	1.22 Fe <sup>2+</sup> + 0.39 Fe <sup>3+</sup> + 0.39 Mn	51.61	2.13	2.13
<i>M</i> (5)	52.0	1.22 Fe <sup>2+</sup> + 0.39 Fe <sup>3+</sup> + 0.39 Mn	51.61	2.13	2.13
<i>M</i> (6)	52.0	1.23 Fe <sup>2+</sup> + 0.77 Mn	51.23	2.17	2.15
<i>M</i> (7)	40.0	1.35 Mn + 0.35 Ca + 0.30 □	40.75	2.24	2.22
<i>M</i> (8)	47.5	1.72 Mn + 0.15 Zn + 0.07 Mg + 0.06 □	48.34	2.19	2.19
<i>M</i> (9)	40.0	1.35 Mn + 0.35 Ca + 0.30 □	40.75	2.24	2.22
Total <i>M</i>	413.5	5.32 Fe <sup>2+</sup> + 4.13 Fe <sup>3+</sup> + 5.97 Mn + 0.70 Ca + 0.15 Zn + 0.07 Mg + 0.66 □	414.29		
<sup>[12]</sup> <i>A</i> (1)	26.6(5)	0.53 K + 0.28 Ba + 0.03 Sr + 0.16 □	26.89		3.17
<sup>[9]</sup> <i>A</i> (2A)	5.2(1.3)				3.19
<sup>[10]</sup> <i>A</i> (2B)	4.5(5)				3.19
<sup>[9]</sup> <i>A</i> (2C)	3.8(5)				3.12
<sup>[9]</sup> <i>A</i> (2D)	5.7(1.3)				3.12
Total <i>A</i> (2)	19.2	1.21 □ + 0.72 K + 0.07 Cs	17.53		3.26
<sup>[10]</sup> <i>B</i>	11.3(4)	1.11 □ + 0.72 Na + 0.17 Ca	11.32		2.72

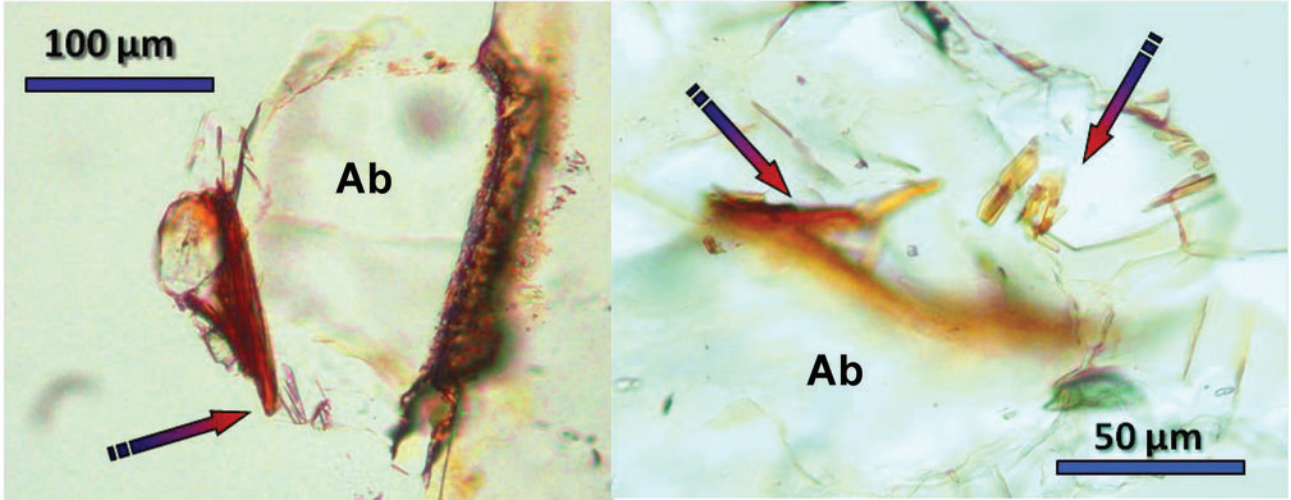
\* X = cation;  $\varphi$  = unspecified anion,  $\varphi$  = O, OH, F, H<sub>2</sub>O;  $\langle X-\varphi \rangle$  calculated using ionic radii of Shannon (1976); \*\* coordination number is shown in brackets for non-octahedral sites.



TABLE 8. continued

Atom	Si(1)	Si(2)	Si(3)	Si(4)	Si(5)	Si(6)	Si(7)	Si(8)	Si(9)	Si(10)	D(1A)	D(1B)	D(2A)	D(2B)	M(1)	M(2)	M(3)	M(4)	M(5)	M(6)	M(7)	M(8)	M(9)	A(1)	B	$\Sigma$
$X_D^O(1)$											0.47	0.22						0.39		0.34			0.32			1.74
$X_D^O(2)$													0.24	0.49					0.40		0.35	0.31				1.71
$^{[3]}X_A^O(1)$																			0.42		0.37	0.36				1.15
$^{[3]}X_A^U(2)$															0.44 <sup>xz</sup> ↓					0.38						1.10
$^{[3]}X_A^O(3)$															0.47		0.45						0.32			1.24
$^{[3]}X_A^O(4)$																	0.53					0.35				1.38
$^{[3]}X_A^O(5)$															0.48		0.37	0.41								1.26
$X_D^P$											0.24	0.67	0.65	0.24											0.06	1.92
																									0.06	
Total	4.10	3.97	4.00	4.13	4.23	4.09	4.08	3.96	4.11	4.28	2.23	2.61	2.62	2.22	2.56	2.53	2.67	2.17	2.22	2.13	1.75	1.88	1.71	0.78	0.57	
Aggr. charge	4.00	4.00	4.00	4.00	4.00	4.00	4.00	4.00	4.00	4.00	2.19	2.45	2.50	2.23	2.67	2.67	2.67	2.20	2.20	2.00	1.70	1.94	1.70	1.15	0.53	

\* Bond-valence parameters are from Brown (1981); coordination numbers are shown for non [4]-coordinated anion; bond-valence values are not calculated from K atoms at the A(2A-2D) sites (~10% occupancy);  $X_A^O(1-5)$  are either O atoms of OH groups or F atoms.



**Fig. 1**

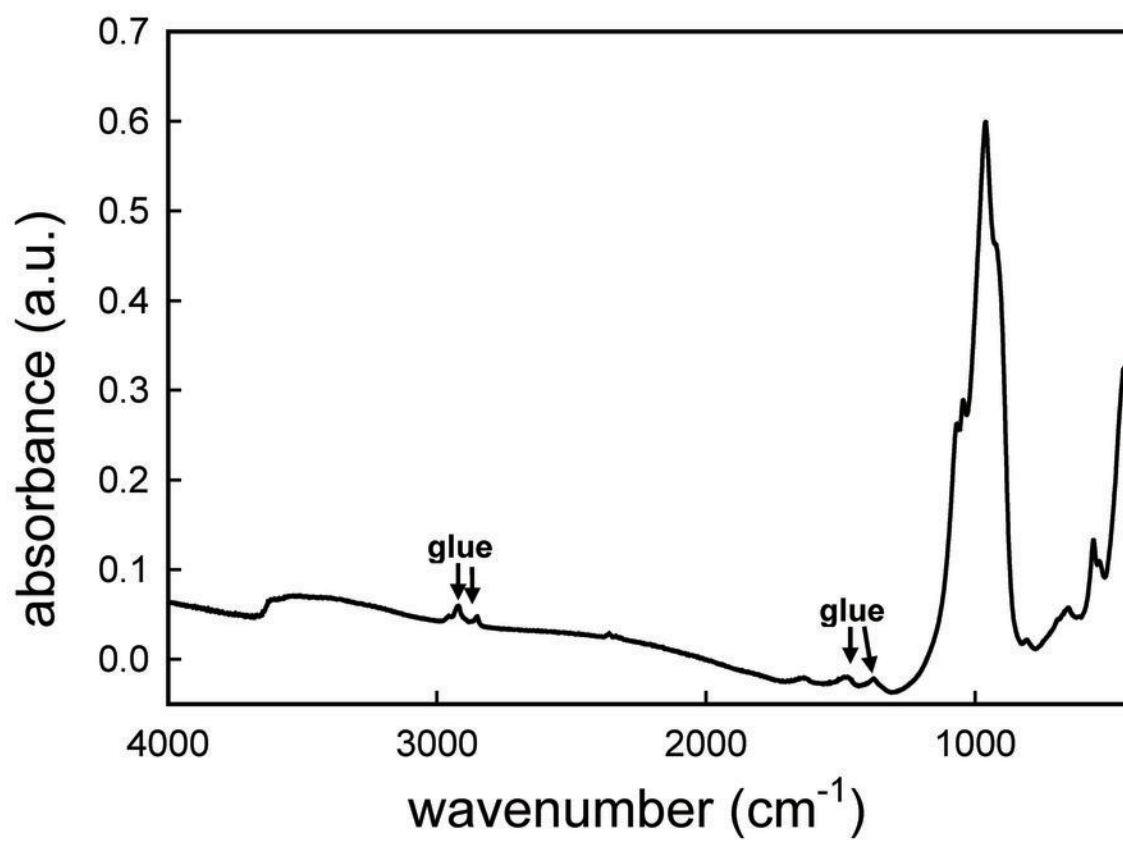


**Fig. 2**

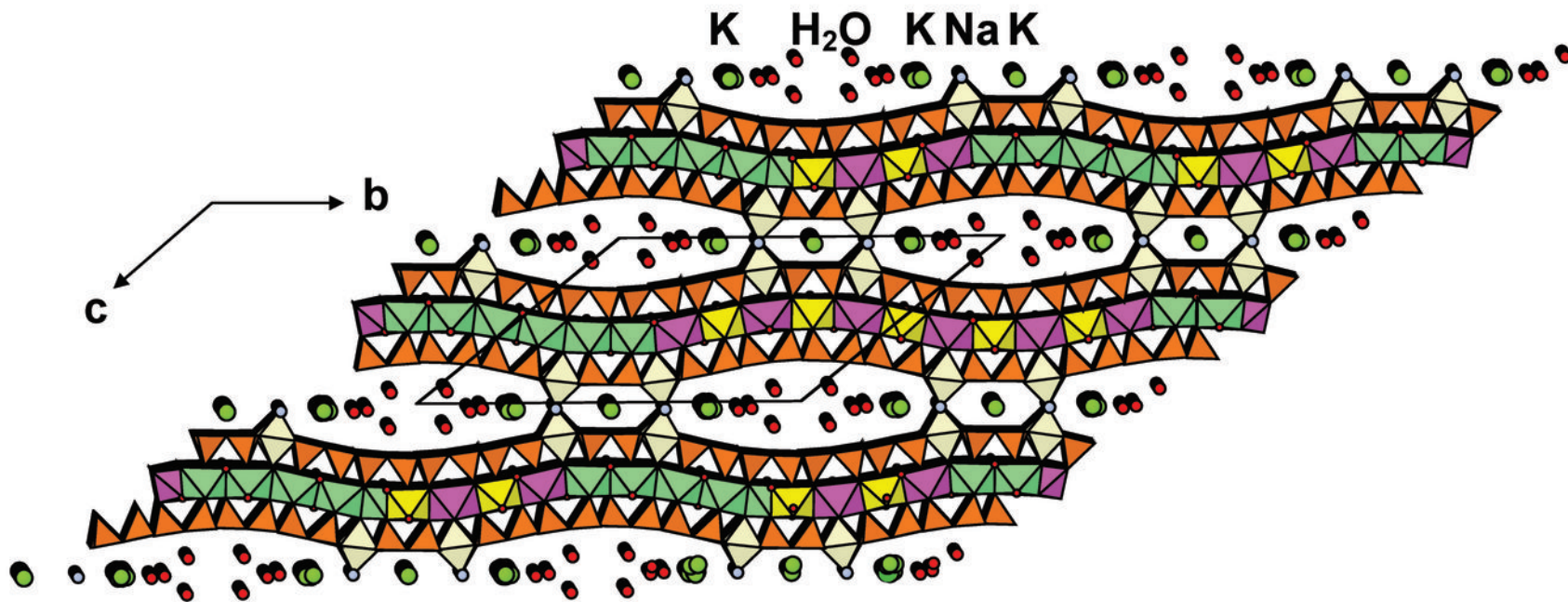
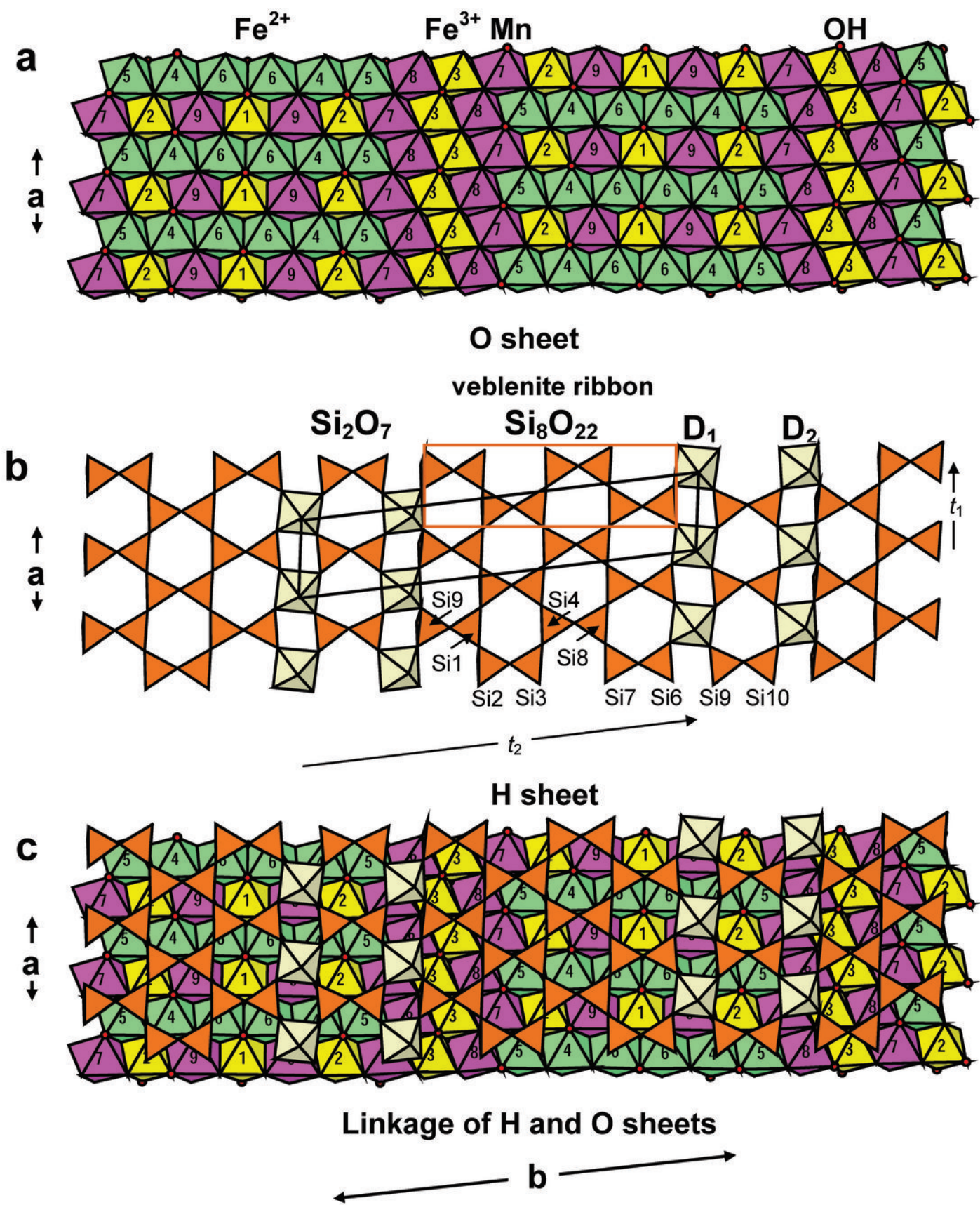


Fig. 3



**Fig. 4**



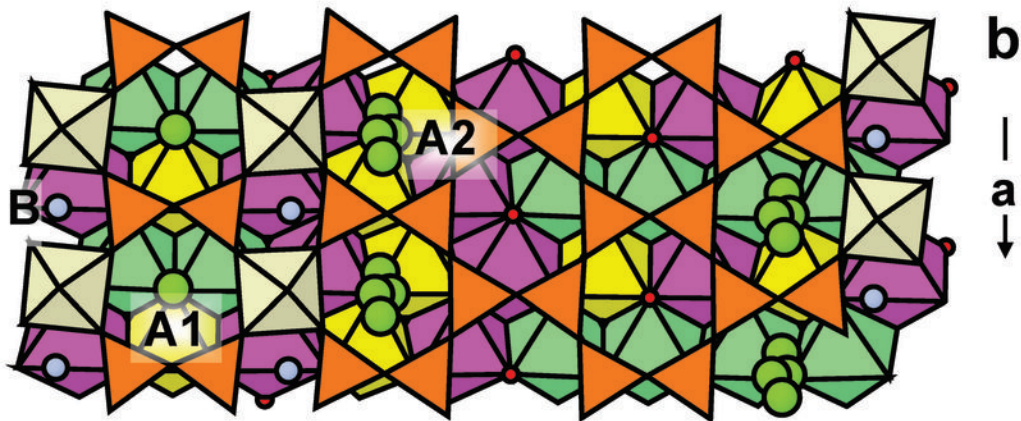
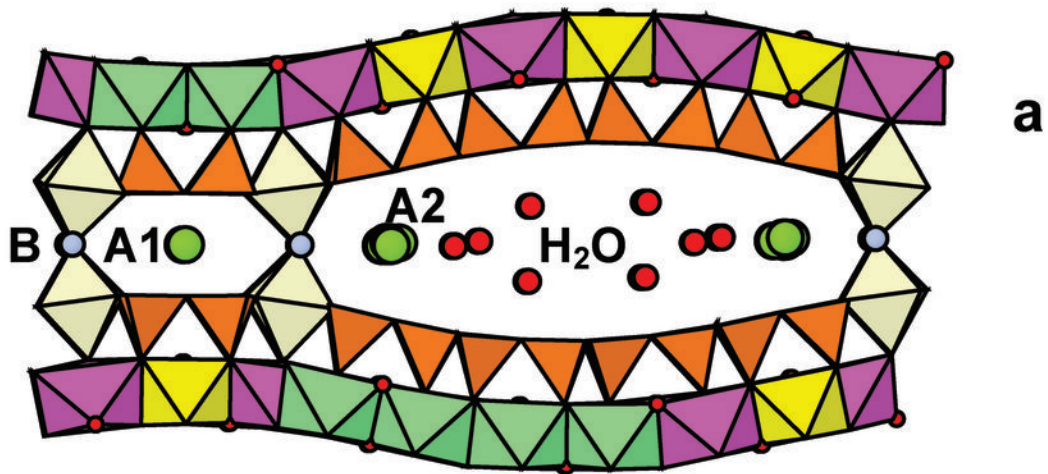


Fig. 5

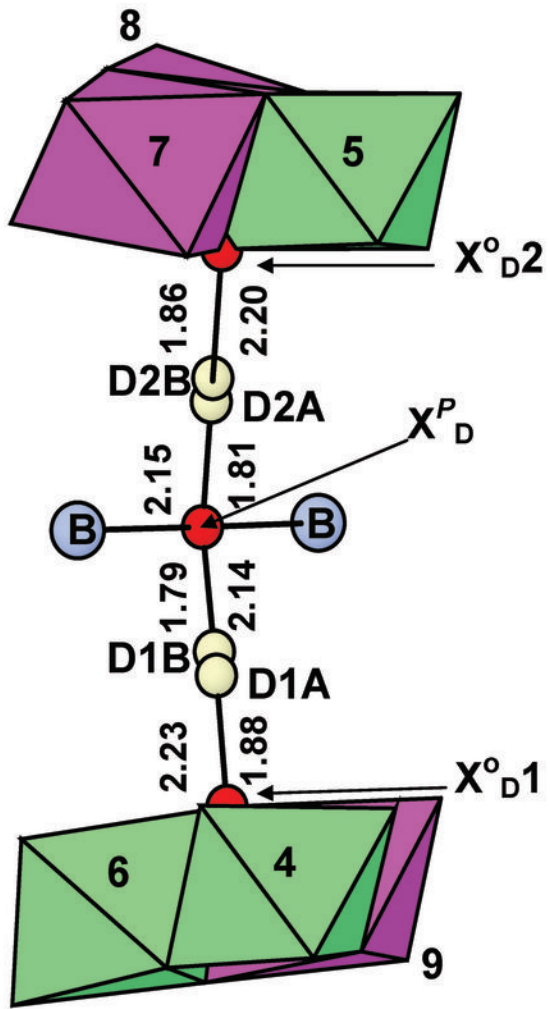


Fig. 6